This is the accepted manuscript made available via CHORUS. The article has been published as:

Modification of Higgs couplings in minimal composite models

Da Liu, Ian Low, and Carlos E. M. Wagner

Phys. Rev. D **96**, 035013 — Published 17 August 2017

DOI: 10.1103/PhysRevD.96.035013

Modification of Higgs Couplings in Minimal Composite Models

Da Liu[a], Ian Low[a,b] and Carlos E. M. Wagner[a,c,d]

[a] *High Energy Physics Division, Argonne National Laboratory, Argonne, IL 60439*
[b] *Department of Physics and Astronomy, Northwestern University, Evanston, IL 60208*
[c] *Enrico Fermi Institute, University of Chicago, Chicago, IL 60637*
[d] *Kavli Institute for Cosmological Physics, University of Chicago, Chicago, IL 60637*

We present a comprehensive study of the modifications of Higgs couplings in the $SO(5)/SO(4)$ minimal composite model. We focus on three couplings of central importance to Higgs phenomenology at the LHC: the couplings to top and bottom quarks and the coupling to two gluons. We consider three possible embeddings of the fermionic partners in **5**, **10** and **14** of $SO(5)$ and find $t\bar{t}h$ and $b\bar{b}h$ couplings to be always suppressed in **5** and **10**, while in **14** they can be either enhanced or suppressed. Assuming partial compositeness, we analyze the interplay between the $t\bar{t}h$ coupling and the top sector contribution to the Coleman-Weinberg potential for the Higgs boson, and the correlation between $t\bar{t}h$ and ggh couplings. In particular, if the electroweak symmetry breaking is triggered radiatively by the top sector, we demonstrate that the ratio of the $t\bar{t}h$ coupling in composite Higgs models over the Standard Model expectation is preferred to be less than the corresponding ratio of the ggh coupling.

I. INTRODUCTION

The discovery of the Higgs boson at the LHC [1, 2] has led to a new era in particle physics. The Standard Model (SM) has been validated as the proper low energy effective theory description of the interactions between the known fundamental particles. The Higgs boson production and decay rates seem to be in good agreement with those predicted in the SM [3], suggesting that the mass generation proceeds from the Higgs mechanism, with the recently discovered Higgs being its observable consequence. The current precision of the Higgs rate measurements, however, leaves some room for departures from the simple SM picture. In particular, data collected at the LHC have only started to probe Higgs couplings with the third generation quarks, which will play a central role in future Higgs measurements, while couplings to fermions in the first two generations remain a challenge. Therefore, it is interesting to study what would be the possible consequences of the deviations of the third generation quark couplings to the Higgs boson and, in particular, what kind of high energy models can accommodate such deviations in a natural way.

A departure from the SM description is to be expected in any model that leads to the breakdown of the electroweak symmetry in a natural way. This could be achieved in models in which the Higgs boson is an elementary or a composite particle. If it is an elementary particle, with renormalizable interactions that remain perturbative until scales of order of the Planck scale, the natural implementation of electroweak symmetry implies a supersymmetric extension that renders the Higgs mass parameter insensitive to the ultraviolet physics [4]. Due to the top-quark contribution to the loop-induced Higgs couplings, any modification of the Higgs coupling to top-quarks [5] will induce a similar modification of its coupling to gluons as measured in terms of their SM values. These two contributions may be rendered independent in the presence of light superpartners of the top-quark (stops) which could contribute in a relevant way to the loop-induced Higgs couplings. Based on this observation, an analysis of the possible enhancement of the Higgs couplings to top-quarks within supersymmetric models was recently presented in Refs. [6, 7].

Alternatively, a natural electroweak symmetry breaking may be achieved by assuming that the Higgs is a composite particle [8–11]. There have been renewed interests in composite Higgs models, following the works in Ref. [12–16], and their interpretations as duals of models of gauge-Higgs unification in warped extra dimensions [17]. In these models, the Higgs appears as a pseudo-Golstone boson and the insensitivity to the ultraviolet scale is ensured by its composite nature, as manifest by its gauge origin in the gauge-Higgs unification picture. The pseudo-Goldstone nature of the Higgs scalar stems from the spontaneous breakdown of a global symmetry group that includes the weak interaction group as a subgroup of it. One of the simplest and most attractive realization is when the global symmetry group is $SO(5)$ [16], which breaks spontaneously into $SO(4)$, that contains both the gauge group $SU(2)_L$, as well as the custodial group $SU(2)_R$. The four Nambu-Goldstone bosons associated with the breaking of the global group are identified with the four components of the Higgs doublet. The properties of the Higgs boson are determined by explicit $SO(5)$ symmetry breaking terms associated with the Yukawa coupling of the third generation quarks, which depend strongly on the representation of $SO(5)$ employed in the fermion sector.

The Higgs couplings in the minimal $SO(5)/SO(4)$ model have been previously studied in the literature [18–22], and it is known that the simplest representation choices lead to a suppression of both the third generation quark and gluon Higgs couplings with respect to the SM ones. In this article, we provide an analytical study of the pattern of the top, bottom and gluon couplings with the Higgs within this minimal model, for different choices of the representations in which the top quark is included. These three couplings are of central importance to the Higgs phenomenology at the LHC. One of our goals is to provide an analytical understanding of the capabilities of this model to fit the future Higgs data. Moreover, we compute the Coleman-Weinberg potential for the Higgs field that is induced by the top quark sector [23, 24] and study the constraints coming from the requirement of obtaining a proper electroweak symmetry breaking (EWSB) with a Higgs mass consistent with the observed one.

The presentation of this article is as follows. In section II we introduce a general framework for computing the relevant Higgs couplings and the Higgs potential by integrating out heavy partners of the third generation quarks in composite Higgs models. In section III we focus on the minimal $SO(5)/SO(4)$ model and analyze the case of introducing composite fermions in the **5** and **10** representation of $SO(5)$. In section IV we analyze the case of employing the **14** representation of $SO(5)$. We reserve section V for our conclusions,. In the Appendices we present some technical overview and details associated with the study. We also briefly discuss the more complicated scenario of using **5** + **10** representations of the $SO(5)$ group in the Appendix.

II. GENERAL ANALYSIS

In this section, we present a general analysis of the relation between the $t\bar{t}h$ and ggh couplings, under broad assumptions that can be applied to arbitrary coset G/H in composite Higgs models. We proceed by integrating out the new TeV scale strong dynamics, which results in an effective Lagrangian containing only SM particles.[1] Effects of the strong dynamics are encoded in terms of the form factors of the SM particles in momentum space, in analogy with the form factors of the nucleons in low-energy QCD. Focusing on the third generation quarks for now, the form factors are defined as:

$$\Pi_{t_L}\ \bar{t}_L \not{p}\ t_L + \Pi_{t_R}\ \bar{t}_R \not{p}\ t_R + \Pi_{b_L}\ \bar{b}_L \not{p}\ b_L + \Pi_{b_R}\ \bar{b}_R \not{p}\ b_R \\ -(\Pi_{t_L t_R}\ \bar{t}_L\ t_R + \Pi_{b_L b_R}\ \bar{b}_L\ b_R + \text{h.c.}) \tag{1}$$

where the form factors are the functions of p^2 and the proto-Yukawa couplings.

We will also assume that SM fermions obtain their masses from linear mixing with the new strong sector according to the hypothesis of *partial compositeness* [25], which means in the UV, we have the mixing Lagrangian:

$$\mathcal{L}_{mix} = (\bar{q}_L)_\alpha (y_L)^\alpha{}_I \mathcal{O}^I_{q_L} + \bar{t}_R (y^t_R)_I \mathcal{O}^I_{t_R} + \bar{b}_R (y^b_R)_I \mathcal{O}^I_{b_R} \tag{2}$$

where the operators $\mathcal{O}^I_i$ from the strong sector furnish some linear representations of G. Note that $\mathcal{L}_{mix}$ must break G explicitly and the proto-Yukawa couplings $y_{L,R}$ can be viewed as spurions parameterizing the effects of the explicit breaking. Then it should be clear that, after integrating out the strong dynamics, the wave function renormalizations $\Pi_{q_{L,R}}$ with $q = t, b$ are proportional to $y^2_{L,R}$, while the mass terms $\Pi_{q_L q_R}$ are proportional to $y_L y_R$. A detailed spurion analysis could put further constraints on the form factors, as will be shown later when we discuss specific embedding of the fermionic partners.

Since we are mainly interested in composite Higgs models in which the Higgs boson is realized as a pseudo-Nambu-Goldstone boson (pNGB), we will further assume that the wave function normalization form factors can be expanded in series of $s^2_h \equiv \sin^2 \frac{h}{f}$, where f is Goldstone boson decay constant:

$$\Pi_{q_L} = \Pi_{0q_L} + s^2_h\ \Pi_{1q_L} + s^4_h\ \Pi_{2q_L} + \cdots , \qquad \Pi_{q_R} = \Pi_{0q_R} + s^2_h\ \Pi_{1q_R} + s^4_h\ \Pi_{2q_R} + \cdots , \tag{3}$$

[1] The current LHC bound on the colored vector-like quark (VLQ) is roughly around 1 TeV (may depend on the branching ratios to SM particles) and in the energy region around the top-quark mass, it is proper to integrate them out.

where $q = t, b$. The expansion follows from the observation that the Higgs boson is a double under $SU(2)_L$ and that there is a shift symmetry acting on the doublet [26]. For the form factors in front of the mass term, if the fermion is embedded in a vectorial representation $\Pi_{q_L q_R} \sim s_{2h} \sim s_h c_h$, while for a spinorial representation it is simply s_h. Since the spinorial representation of the $SO(5)/SO(4)$ model is severely constrained by the precision electroweak measurements [27], we will focus on the vectorial representations and its direct product:

$$\Pi_{q_L q_R} = s_h c_h \left(\Pi_{1 q_L q_R} + s_h^2 \; \Pi_{2 q_L q_R} + \cdots \right) , \tag{4}$$

where $\Pi_{1,2}$ are proportional to the mixing parameters $y_L y_R$.

To compute the Higgs couplings in models where the Higgs is a pNGB, it is important to recall that $\langle h \rangle$ is not the same as the SM Higgs vacuum expectation value of $v = 246$ GeV. Instead, by matching to the W boson mass in the SM one obtains [26]

$$v = f \sin\theta \ , \tag{5}$$

where the misalignment angle θ is defined as $\theta = \langle h \rangle / f$. For $SO(5)/SO(4)$ coset this is explicitly demonstrated in Eq. (A9) of Appendix A. The misalignment angle θ is related to the fine-tuning parameter

$$\xi = \frac{v^2}{f^2} = \sin^2\theta \ , \tag{6}$$

which is commonly employed in the literature. The Higgs coupling measurement at the LHC Run-I requires that ξ should be smaller than 0.2 (mainly coming from hWW, hZZ coupling measurement, see for example Ref. [3]), therefore in the following sections we will take $\xi = 0.1$ and $\xi = 0.2$ as our benchmark values.

The Higgs coupling to fermions can be computed by noting that the fermion masses is computed from the form factors at the zero momentum:

$$m_q = \frac{\Pi_{q_L q_R}(0)}{\sqrt{\Pi_{q_L}(0)}\sqrt{\Pi_{q_R}(0)}} \ , \tag{7}$$

from which we can calculate the $q\bar{q}h$ coupling strength with respect to SM as a function of the form factors:

$$\begin{aligned} c_q \ &\equiv \ \frac{g_{q\bar{q}h}}{(g_{q\bar{q}h})_{\rm SM}} = \frac{v}{m_q}\frac{\partial m_q}{\partial \langle h \rangle} = \sin\theta \frac{\partial}{\partial\theta} \log m_q \\ &= \ \sin\theta \frac{\partial}{\partial\theta} \log \Pi_{q_L q_R} - \frac{1}{2} \sin\theta \frac{\partial}{\partial\theta} \left(\log \Pi_{q_L} + \log \Pi_{q_R} \right) \qquad \text{at} \ \ q^2 = 0 \ . \end{aligned} \tag{8}$$

It turns out that for representations considered in this work, the expansions of the form factors terminate at Π_2 and the $q\bar{q}h$ coupling strength is given by:

$$\begin{aligned} c_q \ &= \ \frac{\cos 2\theta}{\cos\theta} + \frac{2 \ \Pi_{2 q_L q_R} \sin^2\theta \cos\theta}{\Pi_{1 q_L q_R} + \Pi_{2 q_L q_R} \sin^2\theta} \\ &\qquad - \left(\frac{\Pi_{1 q_L} \sin^2\theta \cos\theta + 2 \ \Pi_{2 q_L} \sin^4\theta \cos\theta}{\Pi_{0 q_L} + \Pi_{1 q_L} \sin^2\theta + \Pi_{2 q_L} \sin^4\theta} + L \to R \right) \qquad \text{at} \ \ q^2 = 0 \quad , \end{aligned} \tag{9}$$

where $q = t, b$. Note that the first term is the universal suppression factor coming from the $s_h c_h$ term in the expansion, which can be rewritten in terms of ξ:

$$\frac{\cos 2\theta}{\cos\theta} = \frac{1 - 2\xi}{\sqrt{1-\xi}} \ . \tag{10}$$

Before computing the ggh coupling strength, it is worth recalling the observations made in Refs. [21, 28, 29], which states that, under the assumption of partial compositeness, the determinant of the fermion mass matrix is proportional to the the mass term form factor $\Pi_{q_L q_R}$ at the zero momentum. This is due to the particular form of the mass matrix:

$$-\mathcal{L}_m = (\bar{F}_L, \bar{\vec{\Psi}}_L) M_F(h) \begin{pmatrix} F_R \\ \vec{\Psi}_R \end{pmatrix}, \qquad M_F = \begin{pmatrix} 0 & Y_L^T(h) \\ Y_R(h) & M_c \end{pmatrix}, \tag{11}$$

where F denotes SM fermions and Y_L (Y_R) is the mixing vector in the flavor space between the left-handed (right-handed) SM fermion F and its composite partners. Here M_c is the G-symmetry-preserving mass matrix of the fermionic partners and does not depend on the Higgs field, because in the limit of zero mixing between SM and the composite sector, the G-symmetry is exact and all Higgs interactions must be derivatively coupled. For simplicity, we will assume that all mixing parameters are real and have chosen a basis in the flavor space where M_c is diagonal. It is then not difficult to see:

$$\text{Det}\, M_F = -Y_L^T M_c^{-1} Y_R \;\; \text{Det}\, M_c \tag{12}$$

By integrating out the fermion partners using the equation of motion at the zero momentum from the Lagrangian in Eq. (11), we obtain:

$$\Pi_{F_L F_R}(0) = -Y_L^T M_c^{-1} Y_R \tag{13}$$

which in turn implies:

$$\text{Det}\, M_F = \Pi_{F_L F_R}(0) \;\text{Det}\, M_c \tag{14}$$

Note that the Higgs dependence of the determinant is fully contained in the mass form factor $\Pi_{F_L F_R}(0)$.

In the SM the largest contribution to the ggh coupling comes from the top quark. A detailed discussion of the ggh coupling is given in Appendix B. Here we merely collect the essential results. In the limit of infinite top mass and resonance mass, the charge 2/3 sector contribution to ggh can be obtained:

$$\begin{aligned} c_g^{(2/3)} &\equiv \frac{g_{ggh}^{(2/3)}}{(g_{ggh})_{\text{SM}}} = \sin\theta \frac{\partial}{\partial\theta} \log \Pi_{t_L t_R} \\ &= \frac{\cos 2\theta}{\cos\theta} + \frac{2\;\Pi_{2t_L t_R} \sin^2\theta\cos\theta}{\Pi_{1t_L t_R} + \Pi_{2t_L t_R}\sin^2\theta} \qquad \text{at} \quad q^2 = 0 \;. \end{aligned} \tag{15}$$

For the charge -1/3 sector, the SM bottom quark contributes negligibly to the ggh coupling, which need to be subtracted from the fermion mass matrix of the bottom sector. To be specific, we have:

$$\begin{aligned} c_g^{(-1/3)} &\equiv \frac{g_{ggh}^{(-1/3)}}{(g_{ggh})_{\text{SM}}} = \sin\theta \frac{\partial}{\partial\theta} \left(\log \Pi_{b_L b_R} - \log m_b\right) \\ &= \frac{\Pi_{1b_L}\sin^2\theta\cos\theta + 2\;\Pi_{2b_L}\sin^4\theta\cos\theta}{\Pi_{0b_L} + \Pi_{1b_L}\sin^2\theta + \Pi_{2b_L}\sin^4\theta} \\ &\qquad + \frac{\Pi_{1b_R}\sin^2\theta\cos\theta + 2\;\Pi_{2b_R}\sin^4\theta\cos\theta}{\Pi_{0b_R} + \Pi_{1b_R}\sin^2\theta + \Pi_{2b_R}\sin^4\theta} \qquad \text{at} \quad q^2 = 0 \;. \end{aligned} \tag{16}$$

Note that $c_g^{(-1/3)}$ starts from the linear order in ξ, as we have neglected the SM bottom contribution.

We study the correlation between the ggh and $t\bar{t}h$ couplings by computing

$$\begin{aligned} c_t - c_g &= -\frac{1}{2}\sin\theta\frac{\partial}{\partial\theta}\left(\log\Pi_{t_L} + \log\Pi_{t_R} + \log\Pi_{b_L} + \log\Pi_{b_R}\right) \\ &= -\xi \sum_{q=t,b}\left(\frac{\Pi_{1q_L}}{\Pi_{0q_L}} + \frac{\Pi_{1q_R}}{\Pi_{0q_R}}\right) + \mathcal{O}(\xi^2) \qquad \text{at} \quad q^2 = 0 \;. \end{aligned} \tag{17}$$

Note that if there is no Higgs dependence for all the wave function normalization form factors, c_t is exactly equal to c_g. We will see this limit from the specific calculations for the different representations of $SO(5)/SO(4)$. It turns out, at the leading order in ξ, $c_t - c_g$ has a strong correlation with the fermionic contribution to the Coleman-Weinberg potential of the Higgs boson, which in the Euclidean space is given by [30]

$$V_f(h) = -2N_c \int \frac{d^4Q}{(2\pi)^4}\left[\log\left(Q^2\;\Pi_{t_L}\Pi_{t_R} + |\Pi_{t_L t_R}|^2\right) + \log\left(Q^2\;\Pi_{b_L}\Pi_{b_R} + |\Pi_{b_L b_R}|^2\right)\right] \;. \tag{18}$$

We are only interested in the Higgs potential to the quartic order in s_h:

$$V_f(h) \simeq -\gamma_f\; s_h^2 + \beta_f\; s_h^4 \tag{19}$$

where

$$\gamma_f = \frac{2N_c}{(4\pi)^2}\int_0^{\Lambda^2} dQ^2\;Q^2 \sum_{q=t,b}\left(\frac{\Pi_{1q_L}}{\Pi_{0q_L}} + \frac{\Pi_{1q_R}}{\Pi_{0q_R}} + \frac{1}{Q^2}\frac{\Pi^2_{1q_L q_R}}{\Pi_{0q_L}\Pi_{0q_R}}\right) \;, \tag{20}$$

while β_f is not relevant for present discussion. In the above $\Lambda \sim 4\pi f$ is the cutoff of the composite model. Electroweak symmetry breaking requires

$$\gamma_f > 0 \qquad \text{and} \qquad \beta_f > 0 \ . \tag{21}$$

It turns out that, for the $SO(5)$ embedding of composite resonances studied in this work, the last contribution inside the parenthesis in Eq. (20) is numerically subleading to the first two terms, whose value at $q^2 = 0$ dictates $c_t - c_g$, as can be seen in Eq. (17). As a result, if the integral, Eq. (20), would receive its dominant contribution from the infrared regime, there would be a strong preference for $c_t - c_g > 0$ in order to trigger EWSB. The interrelation between $c_t - c_g$ and γ_f will be studied in details when we consider embeddings of the composite resonances in **5**, **10** and **14** of $SO(5)$.

Notice that γ_f is quadratically divergent. Specifically, from Eq. (1) it is clear that asymptotically in the Euclidean space,

$$\lim_{Q^2\to\infty} \Pi_{q_{L/R}}(Q^2) \sim 1 \ , \qquad \lim_{Q^2\to\infty} \Pi_{q_L q_R}(Q^2) \sim \frac{1}{Q^2} \ , \qquad q = t, b \ . \tag{22}$$

Under the expansion assumed in Eqs. (3) and (4) we see that

$$\lim_{Q^2\to\infty} \Pi_{0q_{L/R}}(Q^2) \sim 1 \ , \qquad \lim_{Q^2\to\infty} \Pi_{1q_{L/R}}(Q^2) \sim \lim_{Q^2\to\infty} \Pi_{1q_L q_R}(Q^2) \sim \frac{1}{Q^2} \ . \tag{23}$$

These considerations suggest the quadratic divergence in γ_f resides only in the first two terms in Eq. (20), while the last term is finite.

In a viable model of natural EWSB, such quadratic divergences must cancel in the Higgs potential. The cancellation of quadratic divergent contributions to γ_f makes the infrared contribution to Eq. (20) more relevant and therefore the correlation between γ_f and $c_t - c_g$ stronger. In what follows we will always impose the cancellation of quadratic divergences in γ_f.

III. 5 AND 10 OF $SO(5)$

In this section, we study the cases where the composite resonances are embedded in the **5** and **10** of $SO(5)$ and mix with the elementary fermions according to Eq. (2). We will see that in neither case can the $t\bar{t}h$ coupling be enhanced over the SM expectation. However, before we begin, it is useful to set up some notation in the CCWZ formalism [31, 32], which will be used heavily in this work. A brief overview of CCWZ can be found in Appendix A.

The main objects of consideration are the Goldstone matrix U and the Goldstone gauge field E_μ, defined in Eqs. (A7) and (A8), respectively. The matrix U transforms under the non-linearly realized $SO(5)$ as:

$$U \to g\ U\ h^\dagger(x) \ , \tag{24}$$

where $g \in SO(5), h(x) \in SO(4)$. Therefore, formally speaking, we can view the U matrix as carrying an $SO(5)$ index on the left and an $SO(4)$ index on the right:

$$U^I_{\ i} \to g^I_{\ J}\ U^J_{\ j}\ h^{\dagger j}_{\ \ i}(x) \ , \tag{25}$$

where we use the capital Roman letters I, J to denote the $SO(5)$ indices and the lower case Roman letters i, j to denote the $SO(4)$ indices. In addition, we choose a basis such that the unbroken $SO(4)$ generators reside in the upper 4×4 block of the $SO(5)$ generators. In this basis $U^I_{\ i}$, $i = 1, \cdots, 4$, can be viewed as an $SO(5)$ vector and an $SO(4)$ vector, while $U^I_{\ 5}$ transforms like an $SO(5)$ vector and an $SO(4)$ singlet. It will be useful to define Σ^I such that

$$\Sigma^I = U^I_{\ 5} = (0, 0, 0, s_h, c_h)^T \ , \qquad \Sigma^\dagger \Sigma = 1 \tag{26}$$

where we have defined $s_h = \sin h/f, c_h = \cos h/f$ and evaluated the Goldstone matrix in the unitary gauge. Σ will play a major role in building $SO(5)$ invariants.

A. 5 of $SO(5)$

We first discuss the case of embedding the composite resonances in the **5** of $SO(5)$ in the top sector. Notice that we assume $SO(5)$ is *explicitly* broken by the mixing of the composite resonances with the elementary fermions. The composite resonances transform as $\mathbf{4}$ ($\Psi_{\mathbf{4}}$) and $\mathbf{1}$ ($\Psi_{\mathbf{1}}$) under $SO(4)$ transformations. The $SO(4)$ is unbroken in the strong sector, but it is also explicitly broken by the elementary-composite mixing. In other words, the mixing explicitly break $SO(5)$ to SM group $SU(2)_L \times U(1)_Y$. In addition, $\mathbf{4}$ decomposes into two $SU(2)_L$ doublets of hypercharge $Y = T^{3R} + X$, which are denoted as $q_T = (T, B)^T_{1/6}$ and $q_{\mathcal{X}} = (\mathcal{X}, \mathcal{T})^T_{7/6}$, where $X = 2/3$ and the subscriptsdenote the hypercharge values. More explicitly,

$$\Psi_{\mathbf{4}} = \frac{1}{\sqrt{2}} \begin{pmatrix} iB - i\mathcal{X} \\ B + \mathcal{X} \\ iT + i\mathcal{T} \\ -T + \mathcal{T} \end{pmatrix} , \qquad \Psi_{\mathbf{1}} = \tilde{T}. \tag{27}$$

The Lagrangian involving the composite fermions is then:

$$\begin{aligned} \mathcal{L}^{M5} &= i\bar{\Psi}_{\mathbf{4}}(\not{D} + i\not{E})\Psi_{\mathbf{4}} - M_4\bar{\Psi}_{\mathbf{4}}\Psi_{\mathbf{4}} + i\bar{\Psi}_{\mathbf{1}}\not{D}\Psi_{\mathbf{1}} - M_1\bar{\Psi}_{\mathbf{1}}\Psi_{\mathbf{1}} \\ &\quad + \left[c_4 y_L f(\bar{q}^5_L)_I U^I{}_i(\Psi_{\mathbf{4}})^i_R + a_4 y_R f(\bar{t}^5_R)_I U^I{}_i(\Psi_{\mathbf{4}})^i_L + h.c.\right] \\ &\quad + \left[c_1 y_L f(\bar{q}^5_L)_I U^I{}_5(\Psi_{\mathbf{1}})_R + a_1 y_R f(\bar{t}^5_R)_I U^I{}_5(\Psi_{\mathbf{1}})_L + h.c.\right] , \end{aligned} \tag{28}$$

where $I = 1, \cdots, 5$ and $i = 1, \cdots, 4$. In the above the first line contains the fermion kinetic and Dirac mass terms, while the second and the third lines contain the mixing terms for $\Psi_{\mathbf{4}}$ and $\Psi_{\mathbf{1}}$, respectively, with the elementary fermions q_L and t_R, which are the explicit realization of the partial compositeness assumption in Eq. (2). In particular, we have "uplifted" the elementary fermions, which only carry $SU(2)_L \times U(1)_Y$ quantum number, to the $SO(5)$ space:

$$q^5_L = \frac{1}{\sqrt{2}} \begin{pmatrix} ib_L \\ b_L \\ it_L \\ -t_L \\ 0 \end{pmatrix} \equiv t_L P_{t_L} + b_L P_{b_L} , \qquad t^5_R = \begin{pmatrix} 0 \\ 0 \\ 0 \\ 0 \\ t_R \end{pmatrix} \equiv t_R P_{t_R} , \tag{29}$$

where we have defined the following projection operators:

$$(P_{t_L})^I = \frac{1}{\sqrt{2}} \begin{pmatrix} 0 \\ 0 \\ i \\ -1 \\ 0 \end{pmatrix}, \quad (P_{b_L})^I = \frac{1}{\sqrt{2}} \begin{pmatrix} i \\ 1 \\ 0 \\ 0 \\ 0 \end{pmatrix}, \quad (P_{t_R})^I = \begin{pmatrix} 0 \\ 0 \\ 0 \\ 0 \\ 1 \end{pmatrix}. \tag{30}$$

In Eq. (28) the c_i and a_i, $i = 1, 4$, are dimensionless parameters that are of order unity. Since we are not going to discuss the CP-violating effects in this paper, we assume these parameters are real.

The projection operators in Eq. (30) can be viewed as spurions carrying an $SO(5)$ index:

$$(P_{t_L})^I \to g^I{}_J (P_{t_L})^J, \qquad (P^\dagger_{t_L})_I \to g^{*J}_I (P^\dagger_{t_L})_J. \tag{31}$$

These properties allow one to construct invariants which formally respect the full $SO(5)$ symmetry of the strong sector. The elementary fermions have the following $U(1)^3_{el}$ global symmetry associated with them:

$$t_{L,R} \to e^{i\alpha_{L,R}} t_{L,R}, \quad P_{t_{L,R}} \to e^{-i\alpha_{L,R}} P_{t_{L,R}}, \quad b_L \to e^{i\beta_L} b_L, \quad P_{b_L} \to e^{-i\beta_L} P_{b_L}. \tag{32}$$

so that the Lagrangian for the composite Higgs has a large global symmetry $\mathcal{G} = SO(5) \times U(1)_X \times U(1)^3_{el}$ where $SO(5)$ is non-linear realized.[2] When we integrate out the composite resonances, the resulting effective Lagrangian preserves this large symmetry $\mathcal{G}$ and, as a consequence, can be constrained by performing a spurion analysis. More specifically, the effective Lagrangian can be constructed out of the following invariants:

$$P^\dagger_{t_L}\Sigma\Sigma^\dagger P_{t_L} = \frac{s_h^2}{2}, \quad P^\dagger_{b_L}\Sigma\Sigma^\dagger P_{b_L} = 0, \quad P^\dagger_{t_R}\Sigma\Sigma^\dagger P_{t_R} = c_h^2, \quad P^\dagger_{t_L}\Sigma\Sigma^\dagger P_{t_R} = -\frac{s_h c_h}{\sqrt{2}} , \tag{33}$$

---

[2] The $U(1)_X$ is required to give the correct hypercharges [16]. The projection operators in Eq. (31) also transform under $U(1)_X$.

where Σ is defined in Eq. (26). This argument implies the wave function form factors in Eq. (1), $\Pi_{t_{L,R}}$, are invariant under $\mathcal{G}$, while $\Pi_{t_L t_R}$ is built out of $P^\dagger_{t_L}$ and P_{t_R} with similar transformation properties under $\mathcal{G}$. In particular, we see Π_{t_L} can only contain a constant term and a term proportional to s_h^2, while there is no dependence on the Goldston bosons (i.e. the Higgs boson) in Π_{b_L}.

The mass eigenstates before EWSB can be obtained by rotating the left-handed fields and right-handed fields with angles $\theta_{L,R}$:

$$\tan\theta_L = \frac{c_4 y_L f}{M_4}, \qquad \tan\theta_R = \frac{a_1 y_R f}{M_1} \tag{34}$$

The mixing matrices will obtain corrections after the Higgs receives a VEV upon EWSB. It is straightforward to obtain the full mass matrices by plugging Eq. (27) and the expression of the Goldstone matrix $U = e^{i\Pi}$ in Eq. (A4) into the Lagrangian in Eq. (28). The result for the charge-2/3 states reads:

$$-\mathcal{L}_{M_{2/3}} = \left(\bar{t}_L, \bar{T}_L, \bar{\mathcal{T}}_L, \bar{\tilde{T}}_L\right) M_{2/3} \begin{pmatrix} t_R \\ T_R \\ \mathcal{T}_R \\ \tilde{T}_R \end{pmatrix}, \qquad M_{2/3} = \begin{pmatrix} 0 & Y_L^T \\ Y_R & M_c \end{pmatrix}, \tag{35}$$

where the mixing vectors Y_L, Y_R and the composite mass matrix M_c are:

$$Y_L = -y_L f \begin{pmatrix} c_4 \frac{1+\cos\theta}{2} \\ c_4 \frac{1-\cos\theta}{2} \\ c_1 \frac{\sin\theta}{\sqrt{2}} \end{pmatrix}, \quad Y_R = y_R f \begin{pmatrix} a_4 \frac{\sin\theta}{\sqrt{2}} \\ -a_4 \frac{\sin\theta}{\sqrt{2}} \\ -a_1 \cos\theta \end{pmatrix}, \quad M_c = \mathrm{diag}(M_4, M_4, M_1). \tag{36}$$

Recall θ is the vacuum misalignment angle defined as $\theta = \langle h\rangle/f$. The dependence on the $\sin\theta, \cos\theta$ in $Y_{L,R}$ can be understood by restoring h to its full $SU(2)_L$ doublet H.

To determine the effects of the composite resonances on the Higgs couplings and the cancellation of quadratic divergences, we need to compute:

$$\begin{aligned} \mathrm{Det} M_{2/3} &= -Y_L^T M_c^{-1} Y_R^* \ \mathrm{Det} M_c \\ &= -\frac{y_L y_R f^2}{\sqrt{2}} \sin\theta\cos\theta \left(\frac{c_4 a_4}{M_4} - \frac{c_1 a_1}{M_1}\right) M_4^2 M_1 , \end{aligned} \tag{37}$$

$$\begin{aligned} \mathrm{Tr}[M_{2/3}^\dagger M_{2/3}] &= 2M_4^2 + M_1^2 + c_4^2 y_L^2 f^2 + a_1^2 y_R^2 f^2 \\ &\quad + \left[\frac{c_1^2 - c_4^2}{2} y_L^2 f^2 + (a_4^2 - a_1^2) y_R^2 f^2\right] \sin^2\theta . \end{aligned} \tag{38}$$

We can see that in the limit $c_4 = c_1, a_1 = a_4, M_1 = M_4$, the mass determinant is zero and the top quark remains massless, since the full $SO(5)$ symmetry is unbroken. On the other hand, in the case of $c_1^2 = c_4^2, a_1^2 = a_4^2$, there is no Higgs dependence in the trace of $M_{2/3}^\dagger M_{2/3}$, which means that the quadratic divergence is cancelled in this limit.

The ggh coupling is obtained by plugging in Eq. (37) into Eq. (B9):

$$\begin{aligned} c_g &= \frac{\cos 2\theta}{\cos\theta} = \frac{1-2\xi}{\sqrt{1-\xi}} \\ &\equiv 1 + \Delta_g \xi + \mathcal{O}(\xi^2) , \qquad \Delta_g = -\frac{3}{2} , \end{aligned} \tag{39}$$

where $\xi = \sin^2\theta = v^2/f^2$. Note that there is no composite mass dependence in the ggh coupling [19, 20]. This can be understood from the fact that there is only one $\mathcal{G}$-invariant that can be constructed out of P_{t_L}, P_{t_R} with Higgs dependence:

$$P^\dagger_{t_L} \Sigma\Sigma^\dagger P_{t_R} = -\frac{s_h c_h}{\sqrt{2}} \tag{40}$$

The determinant of the mass matrix (i.e. the form factor $\Pi_{t_L t_R}(0)$) is then proportional to $P^\dagger_{t_L}\Sigma\Sigma^\dagger P_{t_R}$ and the dependence on the mass scales can only enter through the proportionality constant, which drops out in Eq. (39).

On the other hand, to compute c_t we need to compute the form factors defined in Eq. (1), which can be done by following the procedure of integrating out the composite resonances outlined in Appendix C. In terms of the expansion defined in Eqs. (3) and (4), the form factors are

$$\begin{aligned}
\Pi_{0t_L}(p^2) = \Pi_{0b_L}(p^2) = 1 - \frac{c_4^2 y_L^2 f^2}{p^2 - M_4^2}, \qquad \Pi_{1t_L}(p^2) = \frac{1}{2} y_L^2 f^2 \left(\frac{c_4^2}{p^2 - M_4^2} - \frac{c_1^2}{p^2 - M_1^2} \right) , \\
\Pi_{0t_R}(p^2) = 1 - \frac{a_1^2 y_R^2 f^2}{p^2 - M_1^2}, \qquad \Pi_{1t_R}(p^2) = y_R^2 f^2 \left(-\frac{a_4^2}{p^2 - M_4^2} + \frac{a_1^2}{p^2 - M_1^2} \right) , \\
\Pi_{1t_L t_R}(p^2) = \frac{1}{\sqrt{2}} y_L y_R f^2 \left(\frac{c_4 a_4 M_4}{p^2 - M_4^2} - \frac{c_1 a_1 M_1}{p^2 - M_1^2} \right) ,
\end{aligned} \tag{41}$$

while all other terms vanish. A few comments are in order. First we see the new strong sector contributions to the wave function normalization Π_{t_L} and Π_{t_R} are proportional to y_L^2 and y_R^2, respectively, and that to the mass term $\Pi_{t_L t_R}$ are proportional to $y_L y_R$. In the case where there is no $SO(5)$ breaking effects, i.e. $c_4 = c_1, a_4 = a_1, M_4 = M_1$, all the form factors vanish except the kinetic terms of the SM fermions, which are elementary fermions. On the other hand, in the limit

$$c_4^2 = c_1^2, \qquad a_4^2 = a_1^2 , \tag{42}$$

the form factors $\Pi_{1t_{L,R}}$ vanish asymptotically, which signals the quadratic divergences in the Higgs mass cancel; see the discussion at the end of Sect. II. We will assume this is always the case so that the top quadratic divergence in the Higgs mass is cancelled.

To compute the top mass and the $t\bar{t}h$ coupling, we first evaluate the form factors at the zero momentum:

$$\begin{aligned}
\Pi_{0t_L}(0) = \frac{1}{\cos^2\theta_L}, \quad \Pi_{1t_L}(0) = -\frac{1}{2}\tan^2\theta_L \left(1 - \frac{1}{r_1^2}\right), \quad \Pi_{0t_R}(0) = \frac{1}{\cos^2\theta_R}, \\
\Pi_{1t_R}(0) = -\tan^2\theta_R \left(1 - r_1^2\right), \quad \Pi_{1t_L t_R}(0) = \frac{1}{\sqrt{2}} \frac{c_1}{c_4} M_4 (1 - r_1) \tan\theta_L \tan\theta_R ,
\end{aligned} \tag{43}$$

where we have defined:

$$r_1 = \frac{c_4 a_4}{c_1 a_1} \frac{M_1}{M_4} = \pm \frac{M_1}{M_4} , \tag{44}$$

given our choice of cancellation of quadratic divergences in Eq. (42). In addition, we set $c_1/c_4 = +1$ in the form factor $\Pi_{1t_L t_R}(0)$, because the sign of the fermion mass term is not physical. Now using Eqs. (7) and (8) we obtain m_t and $t\bar{t}h$ coupling:

$$m_t = \frac{1}{\sqrt{2}} M_4 (1 - r_1) \sin\theta \cos\theta \sin\theta_L \sin\theta_R + \cdots , \tag{45}$$

$$\begin{aligned}
c_t &= \frac{\cos 2\theta}{\cos\theta} - \sin^2\theta \cos\theta \left(\frac{\Pi_{1t_L}(0)}{\Pi_{t_L}(0)} + \frac{\Pi_{1t_R}(0)}{\Pi_{t_R}(0)} \right) \\
&\equiv 1 + \Delta_t \xi + \cdots ,
\end{aligned} \tag{46}$$

where we have neglected terms that are higher order in $\xi = \sin^2\theta$ in the top mass. Note that to reproduce the observed top mass for $M_4 \sim 1$ TeV and $\xi \sim 0.1$, we need the mixing parameters $\sin\theta_L \sin\theta_R \sim \mathcal{O}(1)$.

After substituting the form factors in Eq. (43) into Eq. (46), the leading modification in the $t\bar{t}h$ coupling Δ_t is given by

$$\Delta_t = -\frac{3}{2} + \frac{1}{2}\left(1 - \frac{1}{r_1^2}\right) \sin^2\theta_L + \left(1 - r_1^2\right) \sin^2\theta_R \tag{47}$$

$$< \frac{1}{2} \sin^2\theta_L + \sin^2\theta_R - \frac{3}{2} < 0 . \tag{48}$$

Recall that $c_t = 1 + \Delta_t \xi$. We see that Δ_t is always smaller than zero, implying that the $t\bar{t}h$ coupling is always suppressed.[3] In fact, it is possible to strengthen the bound in the above and prove that

$$\Delta_t < -1/2 . \tag{49}$$

---

[3] We also checked that in the limit t_R is fully composite, even though the mass matrix in Eq. (11) has an non-zero first diagonal entry and $Y_R = 0$, $t\bar{t}h$ coupling is still reduced.

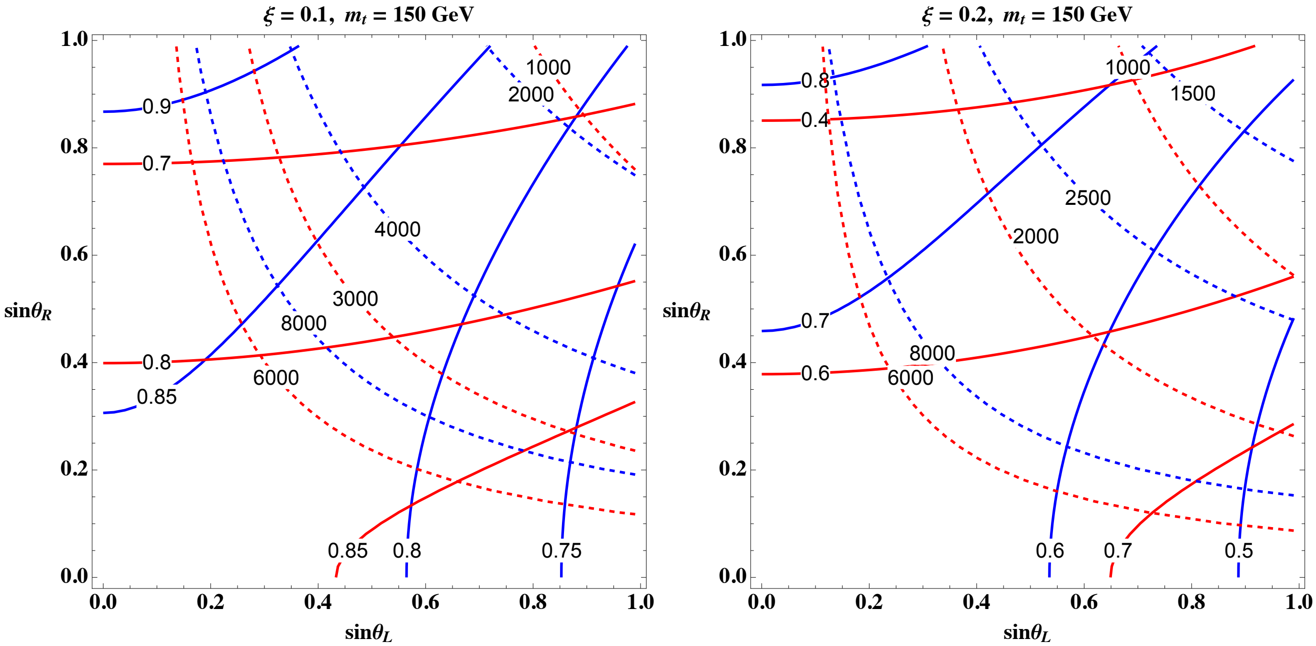

FIG. 1: Contour plots of $t\bar{t}h$ coupling strength c_t (in solid lines) and the mass scale $|M_4|$ in GeV (in dashed lines) with $\xi = 0.1$ (left panel) $\xi = 0.2$ (right panel) and $m_t = 150\,\text{GeV}$ for $r_1 = 0.5$ (in blue) and $r_1 = 2$ (in red). The mass scale M_4 is determined by the full formulae of m_t using Eq. (7) in the case of **5**. We ignore the Higgs potential in this plot.

To see this, we observe from Eqs. (39) and (47) that

$$\begin{aligned}\Delta_t - \Delta_g &= \frac{1}{2}\left(1 - \frac{1}{r_1^2}\right)\sin^2\theta_L + \left(1 - r_1^2\right)\sin^2\theta_R \\ &\leq \left(\frac{|\sin\theta_L|}{\sqrt{2}} - |\sin\theta_R|\right)^2 < 1 \ . \end{aligned} \tag{50}$$

where we have used the identity $a^2 + b^2 \leq 2\sqrt{a^2 b^2}$. Since $\Delta_g = -3/2$ as in Eq. (39), the bound in Eq. (49) follows. It is also worth noting that, in the region $\theta_L \sim \theta_R$, $\Delta_t \approx \Delta_g$:

$$\Delta_t - \Delta_g \ \leq \ \left(\frac{3}{2} - \sqrt{2}\right)\sin^2\theta_{L,R} \ \sim \ 0.1\ \sin^2\theta_{L,R} \ . \tag{51}$$

In Fig. 1 we plot contours of c_t and M_4 as functions of θ_L and θ_R with $\xi = 0.1$ and $m_t = 150$ GeV (taken as a representative value of the running top quark mass at the TeV scale), for different values of r_1.[4] In the figures we always use the full formulas in Eqs. (7) and (8), which captures the full dependence on ξ. For $\xi = 0.1$ the bound in Eq. (49) gives

$$c_t \ \leq \ 0.95 \quad \text{for} \quad \xi = 0.1 \ , \tag{52}$$

which is consistent with the values shown in Fig. 1. Notice that M_4 gives the overall mass scale of the top partners.

Up to now, we have not considered effects of the composite resonances in the Higgs potential. As discussed in Section II , $c_t - c_g$ may be correlated with the coefficient γ_f, defined in Eq. (19), in front of the quadratic term in the potential. Let's define

$$\gamma_f = \frac{2N_c M_4^4}{(4\pi)^2}\int_0^{x_\Lambda} dx\, \mathcal{F}(x) \ , \tag{53}$$

[4] Since the top quark mass is used to determine the value of overall scale M_4 and the dependence is linear, the results are not very sensitive to the exact value of top quark mass (see Eq. (45)).

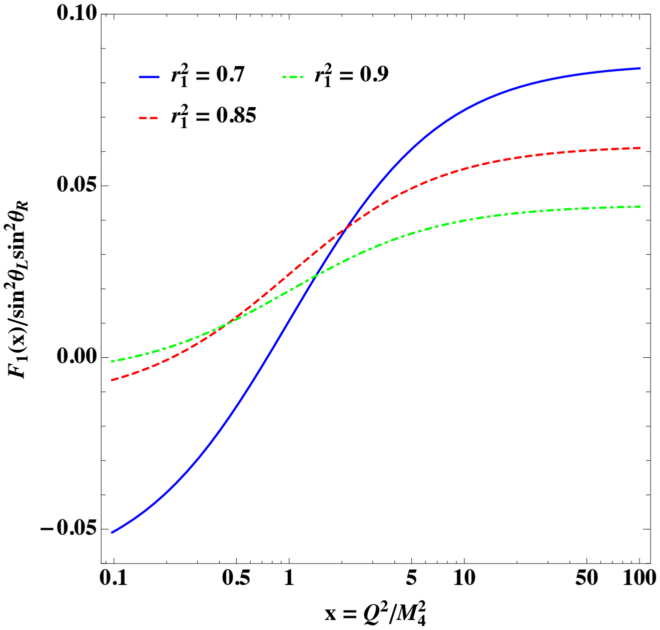

FIG. 2: Plots for $\mathcal{F}_1(x)/\sin^2\theta_L \sin^2\theta_R$ in the case of **5** for different values of r_1^2.

where $x = Q^2/M_4^2, x_\Lambda = \Lambda^2/M_4^2$ and

$$\mathcal{F}(x) = x \sum_{q=t,b} \left(\frac{\Pi_{1q_L}}{\Pi_{0q_L}} + \frac{\Pi_{1q_R}}{\Pi_{0q_R}} + \frac{1}{x} \frac{\Pi^2_{1q_L q_R}}{\Pi_{0q_L}\Pi_{0q_R}} \right) . \tag{54}$$

For the case of **5**, we can obtain

$$\mathcal{F}(x) = \frac{r_1^2 \sec^2\theta_L \sec^2\theta_R}{(x+\sec^2\theta_L)(x+r_1^2\sec^2\theta_R)} \left[-\left(\frac{1}{\xi}(c_t - c_g) + \mathcal{O}(\xi) \right) x + \mathcal{F}_0 + \mathcal{F}_1(x) x \right] , \tag{55}$$

$$\mathcal{F}_0 = \frac{1}{2}\sin^2\theta_L \sin^2\theta_R (1-r_1)^2 = \frac{m_t^2}{\xi M_4^2}(1+\mathcal{O}(\xi)) , \tag{56}$$

$$\mathcal{F}_1(x) = \sin^2\theta_L \sin^2\theta_R (1-r_1^2) \left(1 - \frac{1}{2 r_1^2} - \frac{1}{2}\frac{1}{x+1} \right) , \tag{57}$$

where $\xi = v^2/f^2$ and m_t is given in Eq. (45). Note that in our parametrization, $r_1 = -1$ is the case of the maximally symmetric composite Higgs considered in Ref. [33]. In this limit, all terms in $\mathcal{F}(x)$ vanish except $\mathcal{F}_0$, which is coming from the mass form factor square term in Eq. (54). Note that in this special limit, the dependence on the Higgs field of the wave function normalization form factors disappear, which implies $c_t = c_g$ exactly according to Eq. (17).

It is worth recalling that a sufficient (although not necessary) condition for EWSB is $\mathcal{F}(x) \geq 0$ through out the integration region. Among the three contributions in Eq. (55), $\mathcal{F}_0$ is positive-definite and constant in x. If one chooses $M_4 \sim 1$ TeV and $\xi \sim \mathcal{O}(0.1)$, $\mathcal{F}_0 \lesssim \mathcal{O}(0.5)$ and is numerically small. On the other hand, the first and the last terms in Eq. (55) both grows with x and, therefore, should dominate the integration in γ_f. As can be seen, the first contribution is strongly correlated with $c_t - c_g$. Thus if c_t is larger than c_g in any significant way, one would need a sizeable positive contribution from $\mathcal{F}_1(x)$ to obtain a positive γ_f and EWSB. It turns out that $\mathcal{F}_1(x)$ can be positive only in the region

$$\frac{1}{2} \leq r_1^2 \leq 1 . \tag{58}$$

Even in this region, $\mathcal{F}_1(x)$ is numerically small,

$$\mathcal{F}_1(x) \leq \left(\frac{3}{2} - \sqrt{2} \right) \sin^2\theta_L \sin^2\theta_R \sim 0.086 \ \sin^2\theta_L \sin^2\theta_R , \tag{59}$$

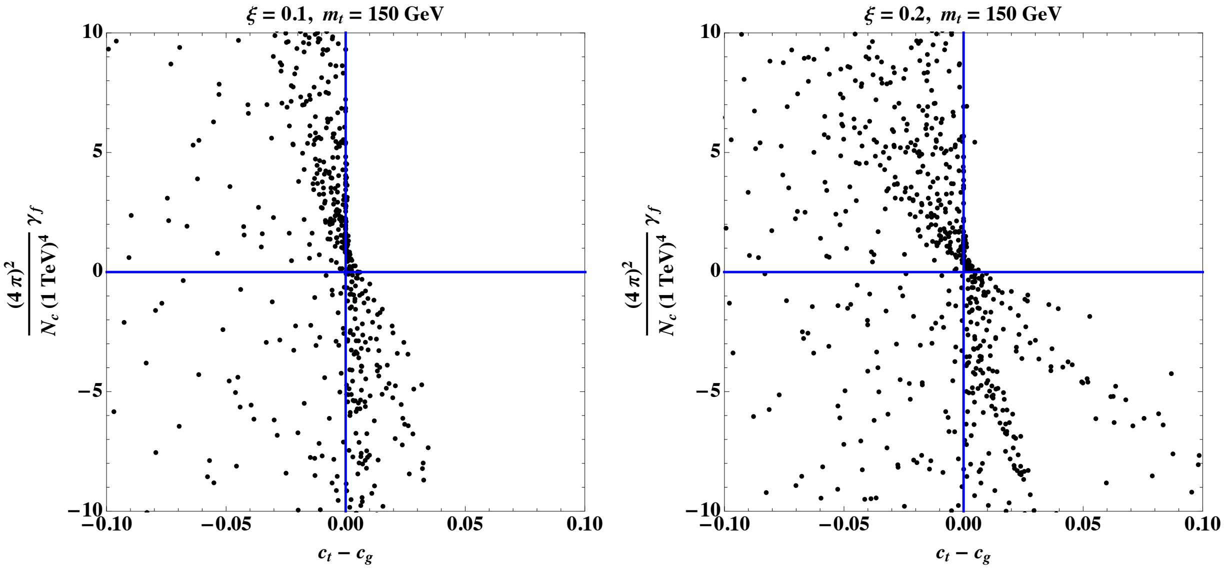

FIG. 3: Scattering plots in the case of **5** for γ_f versus $c_t - c_g$ for $\xi = 0.1$ (left panel) and $\xi = 0.2$ (right panel). We show γ_f in unit of $\frac{N_c}{16\pi^2}(1\,\text{TeV})^4$ and fix the top quark mass $m_t = 150\,\text{GeV}$. We also require that all the scales $(M_4, M_1, , c_4 y_L f, a_1 y_R f)$ are smaller than the cutoff $\Lambda = 4\pi f$ and the lightest top partner is heavier than 1 TeV, i.e. $\text{Min}(|M_4|, \sqrt{M_1^2 + a_1^2 y_R^2 f^2}) > 1\,\text{TeV}$.

In Fig. 2 we plot $\mathcal{F}_1(x)$ normalized to $\sin^2\theta_L \sin^2\theta_R$ for $r_1^2 = 0.7, 0.85$ and 0.9, to demonstrate the bound in Eq. (59).We conclude that the first term in Eq. (55), $-(c_t - c_g)/\xi\, x$, is the dominant contribution to γ_f generically, and that EWSB prefers

$$c_t \ \lesssim \ c_g \ . \tag{60}$$

We will see that this pattern persists considering embeddings in **10** and **14** of $SO(5)$. In Fig. 3 we present numerical scans of γ_f versus $c_t - c_g$ for $\xi = 0.1, 0.2$, confirming the correlation derived from the analytical understanding. In the tiny sliver of region where $c_t > c_g$ and $\gamma_f > 0$, we see $c_t - c_g$ is very small, at the percent level. Note that because the SM gauge boson contribution to the γ factor is always negative, including it will make the preference for $c_t < c_g$ even stronger.

To complete our discussion of the case of **5**, we next discuss the implementation of the bottom Yukawa coupling. In this case we will introduce composite resonances to mix with q_L and b_R, but not t_R. Similar to the top partners, the bottom partners can be embedded in the **5** of $SO(5)$ but with a different $U(1)_X$ charge, $X = -1/3$. This has the effect of mixing q_L with the $T^{3R} = +1/2$ doublet of the composite resonances, as opposed to the $T^{3R} = -1/2$ doublet in the case of the top partner. The projection operators in this case are given by:

$$(P_{t_L})^I = \frac{1}{\sqrt{2}} \begin{pmatrix} -i \\ 1 \\ 0 \\ 0 \\ 0 \end{pmatrix}, \qquad (P_{b_L})^I = \frac{1}{\sqrt{2}} \begin{pmatrix} 0 \\ 0 \\ i \\ 1 \\ 0 \end{pmatrix}, \qquad (P_{b_R})^I = \begin{pmatrix} 0 \\ 0 \\ 0 \\ 0 \\ 1 \end{pmatrix} \tag{61}$$

Because of the similarity of these projection operators to their counter parts in the top sectors, all the formulas for the form factors remain the same except that the mass scales are now for the bottom partners. The leading term for the bottom mass reads:

$$m_b \ = \ \frac{1}{\sqrt{2}}\, M_4^{(b)} \left(1 - r_1^{(b)}\right) \ \sin\theta\cos\theta\sin\theta_L^{(b)}\sin\theta_R^{(b)} \ . \tag{62}$$

Note that in order to reproduce the bottom mass for $M_4^{(b)} \sim 1$ TeV and $\xi \sim 0.1$, we need $\sin\theta_L^{(b)}\sin\theta_R^{(b)} \sim 0.02$. This implies, unless we have a large hierarchy between the left-handed and the right-handed mixing parameters, the contributions to the Higgs potential from the bottom sector can be safely neglected.

Now, by using Eqs. (9) and (16), we obtain

$$\Delta_b = -\frac{3}{2} - \Delta_g^{(b)} \ , \tag{63}$$

$$\Delta_g^{(b)} = -\frac{1}{2}\left(1 - \frac{1}{(r_1^{(b)})^2}\right)\sin^2\theta_L^{(b)} - \left(1 - (r_1^{(b)})^2\right)\sin^2\theta_R^{(b)}, \tag{64}$$

where we have used notations similar to those in the top sector $c_b = 1 + \Delta_b \xi$ and $c_g^{(b)} = \Delta_g^{(b)}\xi$. Since we are neglecting the small SM bottom contribution to the ggh coupling, the bottom partner contribution to ggh coupling in $c_g^{(b)}$ starts at the linear order in ξ. Notice that Δ_b in Eq. (63) has the same expression as Δ_t in Eq. (47), with all the parameters now refer to the bottom sector. Therefore,

$$\Delta_b < -\frac{1}{2} \ . \tag{65}$$

Because the total width of the 125 GeV Higgs boson is dominated by the partial width in the $b\bar{b}$ channel, a reduction in the bottom Yukawa could result an overall increase in the observed signal strength across a variety of channels at the LHC, without modifying the production cross-section in the ggh channel. For example, one can choose so that

$$c_g^{(b)} \sim 0, \qquad c_b \sim \frac{1-2\xi}{\sqrt{1-\xi}} \sim 1 - \frac{3}{2}\xi \ , \tag{66}$$

which implies $c_b \sim 0.85$ for $\xi \sim 0.1$.

B. 10 of $SO(5)$

In this subsection, we embed the composite resonances in the two-index anti-symmetric representation **10** of $SO(5)$, which can be decomposed to $(\mathbf{3},\mathbf{1}) \oplus (\mathbf{1},\mathbf{3}) \oplus \mathbf{4}$ under the unbroken $SO(4)$. Here we assume that the $(\mathbf{3},\mathbf{1})$ and $(\mathbf{1},\mathbf{3})$ have the same mass, which is combined into a **6** under $SO(4)$ and denoted by Ψ^{ij}, with $\Psi^{ij} = -\Psi^{ji}$, for $i, j = 1, \cdots, 4$. We start from the top sector and the effective Lagrangians for the top partner fields:

$$\begin{aligned}\mathcal{L}^{M6_{10}} &= i\bar{\Psi}_{ij}\not{D}\Psi^{ji} - \bar{\Psi}_{ij}\not{E}^{ji}_{\ kl}\Psi^{lk} - M_6\bar{\Psi}_{ij}\Psi^{ji} \\ &\quad + \left[c_6 y_L f\ (\bar{q}_L^{10})_{IJ}U^I_{\ i}U^J_{\ j}\Psi_R^{ji} + a_6 y_R f\ (\bar{t}_R^{10})_{IJ}U^I_{\ i}U^J_{\ j}\Psi_L^{ji} + h.c.\right]\end{aligned} \tag{67}$$

$$\begin{aligned}\mathcal{L}^{M4_{10}} &= i\bar{\Psi}_i\not{D}\Psi^i - \bar{\Psi}_i\not{E}^i_{\ j}\Psi^j - M_4\bar{\Psi}_i\Psi^i \\ &\quad + \sqrt{2}\left[c_4 y_L f\ (\bar{q}_L^{10})_{IJ}U^I_{\ i}U^J_{\ 5}\Psi_R^i + a_4 y_R f\ (\bar{t}_R^{10})_{IJ}U^I_{\ i}U^J_{\ 5}\Psi_L^i + h.c.\right]\end{aligned} \tag{68}$$

where $D_\mu = \partial_\mu + i(2/3)\, B_\mu$. In the limit in which the $c_4 = c_6$, $a_4 = a_6$ and $M_4 = M_6$, the $SO(5)$ invariance is restored. We assign two upper indices to the sixplet composite fields Ψ^{ij} and as a result E_μ will have two upper and two lower indices. The "uplifting" of the elementary fermions q_L and t_R to the $SO(5)$ space in this case is defined by

$$q_L^{10} = t_L P_{t_L} + b_L P_{b_L}, \qquad t_R^{10} = t_R P_{t_R} \ , \tag{69}$$

where

$$\begin{aligned}(P_{t_L})^{IJ} &= \frac{1}{2}\begin{pmatrix} & & & & 0 \\ & & & & 0 \\ & & & & i \\ & & & & -1 \\ 0 & 0 & -i & 1 & \end{pmatrix}, \quad (P_{b_L})^{IJ} = \frac{1}{2}\begin{pmatrix} & & & & i \\ & & & & 1 \\ & & & & 0 \\ & & & & 0 \\ -i & -1 & 0 & 0 & \end{pmatrix}, \\ (P_{t_R})^{IJ} &= \frac{1}{2}\begin{pmatrix} 0 & -i & & & \\ i & 0 & & & \\ & & 0 & -i & \\ & & i & 0 & \\ & & & & 0 \end{pmatrix},\end{aligned} \tag{70}$$

which carry two $SO(5)$ upper indices and will be treated as spurions. Observe that the projection tensors are just the anti-symmetrized version of the product of the embedding vectors in the case of **5**.

Similar to the case of **5**, the spurion analysis reveals only one invariant for each projection operator (keep in mind our contraction convention):

$$\Sigma^T P_q^\dagger P_q \Sigma^* \tag{71}$$

where $q = t_{L,R}$ and $b_{L,R}$. To see this, we observe that the invariant involving the $U^I{}_i$ can always be reduced to the above by using the unitary constraints:

$$U^I{}_i U^{\dagger i}{}_J = \delta^I{}_J - \Sigma^I \Sigma^\dagger_J \ . \tag{72}$$

To be specific, we have:

$$\begin{aligned} \Sigma^T P_{t_L}^\dagger P_{t_L} \Sigma^* &= \frac{1}{2} - \frac{1}{4} s_h^2, \qquad \Sigma^T P_{b_L}^\dagger P_{b_L} \Sigma^* = \frac{1}{2} - \frac{1}{2} s_h^2, \\ \Sigma^T P_{t_R}^\dagger P_{t_R} \Sigma^* &= \frac{1}{4} s_h^2 \ , \qquad \Sigma^T P_{t_L}^\dagger P_{t_R} \Sigma^* = -\frac{1}{4} s_h c_h \end{aligned} \tag{73}$$

which implies the expansion for the form factors in Eq. (3) stops at s_h^2.

Calculating the form factors as before, the form factors for the left-handed sector are

$$\begin{aligned} \Pi_{0t_L}(p^2) &= 1 - \frac{c_4^2 y_L^2 f^2}{p^2 - M_4^2}, \qquad \Pi_{1t_L}(p^2) = \frac{1}{2} y_L^2 f^2 \left(\frac{c_4^2}{p^2 - M_4^2} - \frac{c_6^2}{p^2 - M_6^2} \right) \ , \\ \Pi_{0b_L}(p^2) &= 1 - \frac{c_4^2 y_L^2 f^2}{p^2 - M_4^2}, \qquad \Pi_{1b_L}(p^2) = y_L^2 f^2 \left(\frac{c_4^2}{p^2 - M_4^2} - \frac{c_6^2}{p^2 - M_6^2} \right) \ . \end{aligned} \tag{74}$$

Similarly, for the right-handed sector,

$$\Pi_{0t_R}(p^2) = 1 - \frac{a_6^2 y_R^2 f^2}{p^2 - M_6^2}, \qquad \Pi_{1t_R}(p^2) = \frac{1}{2} y_R^2 f^2 \left(-\frac{a_4^2}{p^2 - M_4^2} + \frac{a_6^2}{p^2 - M_6^2} \right) \tag{75}$$

and the mass term:

$$\Pi_{1t_L t_R}(p^2) = \frac{1}{2} y_L y_R f^2 \left(\frac{c_6 a_6 M_6}{p^2 - M_6^2} - \frac{c_4 a_4 M_4}{p^2 - M_4^2} \right) \ . \tag{76}$$

From the above, we see clearly that Π_{1q} vanishes in the limit $c_6 = c_4$, $a_6 = a_4$ and $M_4 = M_6$, and there is no Higgs dependence in the form factors. This is expected because in this limit the full $SO(5)$ symmetry is restored and the Goldstone field can be rotated away by redefinition of the the composite fields.

Cancellation of quadratic divergence in the top sector requires

$$c_6^2 = c_4^2, \qquad a_6^2 = a_4^2 \ , \tag{77}$$

but not $M_4^2 = M_6^2$, since the mass term only breaks $SO(5)$ "softly." We assume Eq. (77).

We also define the following useful parameters

$$\tan\theta_L = \frac{c_4 y_L f}{M_4}, \qquad \tan\theta_R = \frac{a_6 y_R f}{M_1}, \qquad r_6 = \frac{c_4 a_4}{c_6 a_6} \frac{M_6}{M_4} = \pm \frac{M_6}{M_4} \ . \tag{78}$$

Now it is straightforward to obtain the top mass at the leading order in ξ,

$$m_t = \frac{1}{2} M_4 \left(1 - r_6\right) \ \sin\theta \cos\theta \sin\theta_L \sin\theta_R \ , \tag{79}$$

which is the same as in the case of **5** except the 1/2 factor in front. The modifications to the $t\bar{t}h$ and ggh couplings from the top sector are then:

$$\Delta_g^{(t)} = -\frac{3}{2} + \left(\frac{1}{r_6^2} - 1 \right) \sin^2\theta_L, \tag{80}$$

$$\begin{aligned} \Delta_t &= -\frac{3}{2} + \frac{1}{2} \sin^2\theta_L \left(1 - \frac{1}{r_6^2} \right) + \frac{1}{2} \sin^2\theta_R \left(1 - r_6^2 \right) \\ &< -\frac{3}{2} + \frac{1}{2} (|\sin\theta_L| - |\sin\theta_R|)^2 < -1 \ , \end{aligned} \tag{81}$$

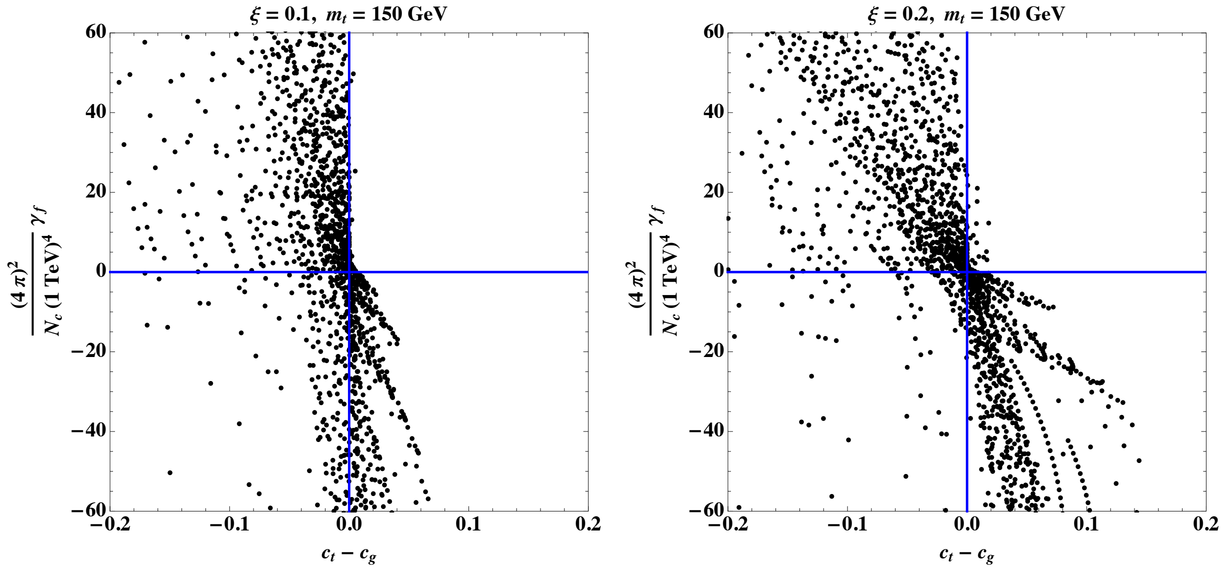

FIG. 4: Scattering plots in the case of **10** for γ_f versus $c_t - c_g$ for $\xi = 0.1$ (left panel) and $\xi = 0.2$ (right panel). We show γ_f in unit of $\frac{N_c}{16\pi^2}(1\,\text{TeV})^4$ and fix the top mass $m_t = 150\,\text{GeV}$, which is obtained by choosing the appropriate value of M_4. We also require that all the scales $(M_4, M_6, , c_4 y_L f, a_6 y_R f)$ are smaller than the cutoff $\Lambda = 4\pi f$ and the lightest top partner is heavier than 1 TeV, i.e. $\text{Min}(|M_4|, \sqrt{M_6^2 + a_1^2 y_R^2 f^2}) > 1\,\text{TeV}$.

where we have used the same convention for the Δ's as in the case of **5**. We see immediately that 1) $c_g = 1 + \Delta_g^{(t)}\xi$ can be either enhanced or reduced and 2) the top Yukawa coupling is not only always suppressed, but the suppression is in general stronger than in the case of **5**. On the other hand,

$$\begin{aligned} \Delta_t - \Delta_g^{(t)} &= \frac{3}{2}\sin^2\theta_L\left(1 - \frac{1}{r_6^2}\right) + \frac{1}{2}\sin^2\theta_R\left(1 - r_6^2\right) \\ &< \frac{1}{2}\left(\sqrt{3}\,|\sin\theta_L| - |\sin\theta_R|\right)^2 < \frac{3}{2}\ . \end{aligned} \tag{82}$$

As for the Higgs potential, we compute $\mathcal{F}(x)$ in Eq. (53):

$$\mathcal{F}(x) = \frac{r_6^2\sec^2\theta_L\sec^2\theta_R}{(x + \sec^2\theta_L)(x + r_6^2\sec^2\theta_R)}\left[-\left(\frac{1}{\xi}(c_t - c_g) + \mathcal{O}(\xi)\right)\,x + \mathcal{F}_0 + \mathcal{F}_1(x)x\right]\ , \tag{83}$$

where

$$\mathcal{F}_0 = \frac{1}{4}\sin^2\theta_L\sin^2\theta_R(1 - r_6)^2 = \frac{m_t}{\xi M_4^2}\left(1 + \mathcal{O}(\xi)\right)\ , \tag{84}$$

$$\mathcal{F}_1(x) = \frac{1}{2}\sin^2\theta_L\sin^2\theta_R(1 - r_6^2)\left[1 - \frac{3}{r_6^2} - \frac{1}{2}\frac{1}{x+1} + \frac{5}{2}\frac{1}{x + r_6^2}\right]\ . \tag{85}$$

Notice that $\mathcal{F}(x)$ has a similar structure to the case of **5**, where $\mathcal{F}_0$ is related to the top mass and expected to be subdominant for $M_4 \sim 1$ TeV and $\xi \sim \mathcal{O}(0.1)$. As for $\mathcal{F}_1(x)$, one can show that it is positive only in the region

$$1 < r_6^2 < 3\ . \tag{86}$$

In this region it is possible to demonstrate that

$$\mathcal{F}_1(x) \leq 0.26\ \sin^2\theta_L\sin^2\theta_R\ . \tag{87}$$

So again there is a strong preference for $c_t < c_g$ in order to trigger EWSB, which is confirmed in the numerical scan shown in Fig. 4.

For the bottom sector, we again introduce composite fermions that mix with b_R but not t_R, which is similar to the case of **5** and the results for the modifications of ggh coupling and $hb\bar{b}$ coupling read:

$$\Delta_b = -\frac{3}{2} - \Delta_g^{(b)} \ , \tag{88}$$

$$\Delta_g^{(b)} = -\sin^2\theta_L^{(b)}\left(1 - \frac{1}{(r_6^{(b)})^2}\right) - \sin^2\theta_R^{(b)}\left(1 - (r_6^{(b)})^2\right), \tag{89}$$

Again Δ_b is similar to its corresponding expression of Δ_t in Eq. (81). As a result, the same bound

$$\Delta_b < -1 \tag{90}$$

applies. Also similar to the case of **5**, if we assume that the mixing parameters in the bottom sector are small, it is possible to modify the $b\bar{b}h$ coupling without chaning the ggh coupling, as done in Eq. (66).

IV. 14 OF $SO(5)$

14 is the two-index symmetric-traceless representation of $SO(5)$. This scenario is distinct from the cases of **5** and **10** in that there are two non-trivial $SO(5)$ invariants one can construct in the spurion analysis. As a result, the ggh coupling now has a non-trivial dependence on the mass of the composite resonance [28] and, moreover, the $t\bar{t}h$ coupling can be enhanced. A qualitatively similar, but numerically more complicated, scenario of embedding the composite fermions in $\mathbf{5}+\mathbf{10}$ simultaneously is discussed in Appendix D.

A. The Top Sector

Under the unbroken $SO(4) \simeq SU(2)_L \times SU(2)_R$, **14** can be decomposed into $\mathbf{9}\oplus\mathbf{4}\oplus\mathbf{1} \simeq (\mathbf{3},\mathbf{3})\oplus(\mathbf{2},\mathbf{2})\oplus\mathbf{1}$. Therefore we introduce three mass scales, M_9, M_4 and M_1 for the 9-plet, 4-plet and the singlet, respectively. The uplifting of the elementary fermion to the $SO(5)$ space achieved through the following projection operators:

$$q_L^{14} = t_L P_{t_L} + b_L P_{b_L} \ , \quad t_R^{14} = t_R P_{t_R} \ , \tag{91}$$

$$(P_{t_L})^{IJ} = \frac{1}{2}\begin{pmatrix} & & & & 0 \\ & & & & 0 \\ & & & & i \\ & & & & -1 \\ 0 & 0 & i & -1 & \end{pmatrix}, \quad (P_{b_L})^{IJ} = \frac{1}{2}\begin{pmatrix} & & & & i \\ & & & & 1 \\ & & & & 0 \\ & & & & 0 \\ i & 1 & 0 & 0 & \end{pmatrix},$$
$$(P_{t_R})^{IJ} = \frac{1}{2\sqrt{5}}\begin{pmatrix} -1 & & & & \\ & -1 & & & \\ & & -1 & & \\ & & & -1 & \\ & & & & 4 \end{pmatrix}. \tag{92}$$

These projection operators carry two $SO(5)$ indices, which are just the symmeterized version of the tensor product of two projection operators in the case of **5**.

The effective Lagrangians for the top partner fields:

$$\mathcal{L}^{M9_{14}} = i\bar{\Psi}(\not{D} + i\not{E})\Psi - M_9\bar{\Psi}_{ij}\Psi^{ji} + \left[c_9 y_L f(\bar{q}_L^{14})_{IJ} U^I_{\ i} U^J_{\ j}\Psi_R^{ji} + a_9 y_R f(\bar{t}_R^{14})_{IJ} U^I_{\ i} U^J_{\ j}\Psi_L^{ji} + h.c.\right] \tag{93}$$

$$\mathcal{L}^{M4_{14}} = i\bar{\Psi}(\not{D} + i\not{E})\Psi - M_4\bar{\Psi}\Psi + \sqrt{2}\left[c_4 y_L f(\bar{q}_L^{14})_{IJ} U^I_{\ i} U^J_{\ 5}\Psi_R^i + a_4 y_R f(\bar{t}_R^{14})_{IJ} U^I_{\ i} U^J_{\ 5}\Psi_L^i + h.c.\right] \tag{94}$$

$$\mathcal{L}^{M1_{14}} = i\bar{\Psi}\not{D}\Psi - M_1\bar{\Psi}\Psi + \frac{\sqrt{5}}{2}\left[c_1 y_L f(\bar{q}_L^{14})_{IJ} U^I_{\ 5} U^J_{\ 5}\Psi_R + a_1\, y_R f(\bar{t}_R^{14})_{IJ} U^I_{\ 5} U^J_{\ 5}\Psi_L + h.c.\right] \tag{95}$$

where $D_\mu = \partial_\mu + i2/3\, B_\mu$ and the numerical factors in front of the mixing terms are such that, in the limit in which $c_1 = c_4 = c_9$, $a_1 = a_4 = a_9$, and $M_1 = M_4 = M_9$, the full $SO(5)$ symmetry is recovered. Notice that, in the above, the 9-plet fermion Ψ^{ij} is a symmetric, traceless rank-2 tensor field with $i,j = 1, \cdots, 4$, which means that only the traceless part of $(\bar{q}_L^{14})_{IJ} U^I_{\ i} U^J_{\ j}, (\bar{t}_R^{14})_{IJ} U^I_{\ i} U^J_{\ j}$ mixing with it. The corresponding E_μ in the kinetic term therefore has two upper and two lower indices.

Similar to the case of **5**, the 4-plet can be decomposed as two $SU(2)_L$ doublets which are denoted as $q_T = (T, B)_{1/6}$ and $q_X = (X_{5/3}, X_{2/3})_{7/6}$; see Eq. (27). For the 9-plet, it can be decomposed as three degenerate $SU(2)_L$ triplets ($I_L = 1$) with hypercharge $5/3, 2/3, -1/3$ respectively. From these quantum numbers we see, before EWSB, the triplet fermions and q_X cannot mix with the elementary fermions, while q_T and the singlet $\tilde{T}$ can mix with the q_L and t_R, respectively, which is similar to the case of **5**. The mass spectrum before EWSB is then

$$M_\psi = M_9, \quad M_T = \sqrt{M_4^2 + c_4^2 y_L^2 f^2}, \quad M_X = M_4, \quad M_{\tilde{T}} = \sqrt{M_1^2 + a_1^2 y_R^2 f^2}\ , \tag{96}$$

where $M_\psi, M_T, M_X, M_{\tilde{T}}$ are the masses of the triplets, the doublet q_T, the doublet q_X and the singlet respectively. After EWSB, the physical masses will be corrected at $\mathcal{O}(\xi)$, except the exotic electric charge $(8/3, 5/3, -4/3)$ states. We then define the following mixing parameters:

$$\tan\theta_L = \frac{c_4 y_L f}{M_4}, \qquad \tan\theta_R = \frac{a_1 y_R f}{M_1}\ , \tag{97}$$

which is similar to the case of **5**.

As in previous cases, we first explore the independent $SO(5)$ invariants involving the Goldstone matrix and the projection operators in Eq. (92). A useful observation in this regard is the fact that an invariant involving the $U^I_{\ i}$ can be rewritten by using the unitary constraints:

$$U^I_{\ i} U^{\dagger i}_{\ \ J} = \delta^I_{\ J} - \Sigma^I \Sigma^\dagger_J\ . \tag{98}$$

As a result, the following decomposition applies

$$(P_q^\dagger)_{IJ} U^I_{\ i} U^J_{\ 5} U^{\dagger i}_{\ \ K} U^{\dagger 5}_{\ \ L} (P_q)^{KL} = \Sigma^T P_q^\dagger P_q \Sigma^* - \Sigma^T P_q^\dagger \Sigma\ \Sigma^\dagger P_q \Sigma^*\ . \tag{99}$$

In the end there are precisely two and only two invariants for the form

$$\Sigma^T P_q^\dagger P_q \Sigma^*, \qquad \Sigma^T P_q^\dagger \Sigma\ \Sigma^\dagger P_q \Sigma^* \tag{100}$$

where here P_q generally denotes $P_{t_{L,R}}, P_{b_{L,R}}$.

An important consequence of having two different $SO(5)$ invariants is that now we have two Higgs-dependent terms in the $\Pi_{t_L t_R}$ and, as a result, the ggh coupling depends on the composite mass scales, unlike in the case of **5** and **10**. To be specific, we have:

$$\Sigma^T P_{t_L}^\dagger P_{t_R} \Sigma^* = -\frac{3}{4\sqrt{5}} s_h c_h, \qquad \Sigma^T P_{t_L}^\dagger \Sigma\ \Sigma^\dagger P_{t_R} \Sigma^* = \left(-\frac{2\sqrt{5}}{5} + \frac{\sqrt{5}}{2} s_h^2\right) s_h c_h \tag{101}$$

which implies the mass form factor now contains two different trigonometric combinations: $s_h c_h$ and $s_h^3 c_h$. In other words, $\Pi_{2q_L q_R}$ is now non-vanishing in Eq. (4). A similar computation for the form factors Π_{t_L} and Π_{t_R} shows that they contain expansion up to $\mathcal{O}(s_h^4)$, while the expansion in Π_{b_L} stops at s_h^2 because $\Sigma^T P_{b_L}^\dagger \Sigma = 0$. In the end, the form factors in the case of **14** have the following expansions,

$$\begin{aligned} \Pi_{t_L} &= \Pi_{0t_L} + s_h^2 \Pi_{1t_L} + s_h^4 \Pi_{2t_L}, \quad \Pi_{t_R} = \Pi_{0t_R} + s_h^2 \Pi_{1t_R} + s_h^4 \Pi_{2t_R}, \\ \Pi_{b_L} &= \Pi_{0b_L} + s_h^2 \Pi_{1b_L}, \qquad\qquad \Pi_{t_L t_R} = s_h c_h \left(\Pi_{1t_L t_R} + s_h^2 \Pi_{2t_L t_R}\right). \end{aligned} \tag{102}$$

Similar to previous cases, cancellation of quadratic divergences in the top sector requires the following condition,

$$c_9^2 = c_4^2 = c_1^2, \quad a_9^2 = a_4^2 = a_1^2\ , \tag{103}$$

which we impose in our analysis. Furthermore, we define

$$r_1 = \frac{c_4 a_4}{c_1 a_1} \frac{M_1}{M_4} = \pm \frac{M_1}{M_4}, \qquad r_9 = \frac{c_4 a_4}{c_9 a_9} \frac{M_9}{M_4} = \pm \frac{M_9}{M_4}\ . \tag{104}$$

Now it is straightforward to obtain the top mass from the form factors:

$$m_t = \frac{\sqrt{5}}{2} M_4 \left(1 - r_1\right) \ \sin\theta\cos\theta\sin\theta_L\sin\theta_R \tag{105}$$

where again we have neglected the higher order terms in $\xi = \sin^2\theta$. Notice the above formula is the same as the case of **5** except the numerical factor $\sqrt{5}/2$. One relevant difference with respect to the **5** and **10** cases is that the top-quark mass dependence on ξ include higher order terms which are proportional to $(1-r_9)$ and not to $(1-r_1)$. This implies that for $r_1 \to 1$, the dominant dependent of the top-quark mass is not linear on the Higgs field, what makes it difficult to generate a realistic top mass and a light Higgs boson at the same time, and also causes an unacceptably large departure of the top-quark coupling to the Higgs with respect to its SM value. Hence, a phenomenologically viable model can only be obtained if the leading contribution proportional to $(1 - r_1)$, Eq. (105), is sizable compared to the higher order terms proportional to $(1 - r_9)$. The formulae below are derived under this assumption.

By following the same calculation as in before, we obtain the modifications to the $t\bar{t}h$ and ggh couplings:

$$\Delta_g^{(t)} \;=\; -4 - \frac{3}{2}\frac{1-1/r_9}{1-1/r_1} + \left(\frac{1}{r_9^2} - 1\right)\sin^2\theta_L \ , \tag{106}$$

$$\begin{aligned}\Delta_t \;&=\; -4 - \frac{3}{2}\frac{1-1/r_9}{1-1/r_1} + \frac{5}{4}\sin^2\theta_L\left[\left(1 - \frac{1}{r_9^2}\right) + \left(1 - \frac{1}{r_1^2}\right)\right] \\ &\quad + \frac{5}{2}\sin^2\theta_R\left(1 - r_1^2\right) \ ,\end{aligned} \tag{107}$$

where $c_t = 1 + \Delta_t\xi$ and $c_g^{(t)} = 1 + \Delta_g^{(t)}\xi$. The superscript in $\Delta_g^{(t)}$ indicates this is the contribution from the top sector. Notice that, in Eqs. (106) and (107), there is a fictitious pole at $r_1 = 1$, which is just a reflection of our previously stated approximation of keeping only the leading contribution in ξ to the top quark mass, Eq. (105). Again, such a fictitious pole does not arise in the case of **5** and **10** because in these two cases Δ_g and Δ_t do not have explicit dependence on the composite scales.

Let's analyze the ggh and $t\bar{t}h$ couplings without considering the Higgs potential, for now. The most important distinctions from the cases of **5** and **10** is that, in the current scenario, Δ_g and Δ_t can be either positive or negative. In other words, there are enough degrees of freedom in Eqs. (106) and (107) such that c_g and c_t could be either enhanced or reduced. It is easiest to demonstrate this numerically. In Fig. 6 we plot contours of c_g and c_t for the benchmark of $\xi = 0.1$ and $\sin\theta_L = \sin\theta_R = 0.8$ (left panel), $\sin\theta_L = 0.3, \sin\theta_R = 0.9$ (right panel), where it is clear that they can be enhanced or reduced over the SM expectations for the reasonable values of $|M_4|$, which is the overall mass scale for the top partners.

Next let's turn to the difference between the $t\bar{t}h$ and ggh couplings, which is given by:

$$\Delta_t - \Delta_g = \frac{1}{4}\sin^2\theta_L\left(14 - \frac{9}{r_9^2} - \frac{5}{r_1^2}\right) + \frac{5}{2}\sin^2\theta_R\left(1 - r_1^2\right) \tag{108}$$

It is evident that:

$$\begin{aligned}\Delta_t - \Delta_g &< \frac{1}{4}\sin^2\theta_L\left(14 - \frac{5}{r_1^2}\right) + \frac{5}{2}\sin^2\theta_R\left(1 - r_1^2\right) \\ &< \frac{7}{2}\sin^2\theta_L + \frac{5}{2}\sin^2\theta_R - \frac{5}{\sqrt{2}}|\sin\theta_L\sin\theta_R|\end{aligned} \tag{109}$$

from which we can see that:

$$\Delta_t - \Delta_g < \frac{7}{2} \tag{110}$$

Again this quantity enters into the Higgs potential through Eq. (53),

$$\mathcal{F}(x) = \frac{r_1^2\sec^2\theta_L\sec^2\theta_R}{(x+\sec^2\theta_L)(x+r_1^2\sec^2\theta_R)}\left[-\left(\frac{1}{\xi}(c_t - c_g) + \mathcal{O}(\xi)\right)\ x + \mathcal{F}_0 + \mathcal{F}_1(x)x\right] \tag{111}$$

where:

$$\mathcal{F}_0 \;=\; \frac{5}{4}\sin^2\theta_L\sin^2\theta_R(1-r_1)^2 = \frac{m_t^2}{\xi M_4^2}\left(1 + \mathcal{O}(\xi)\right) \ , \tag{112}$$

$$\begin{aligned}\mathcal{F}_1(x) \;&=\; \frac{9}{4}\sin^2\theta_L(1-r_9^2)\left(\frac{\cos^2\theta_R}{r_1^2} - \frac{1}{r_9^2}\right)\left(1 - \frac{r_9^2}{x+r_9^2}\right) \\ &\quad + \frac{5}{2}\sin^2\theta_L\sin^2\theta_R(1-r_1^2)\left(1 - \frac{1}{2\,r_1^2} - \frac{1}{2}\frac{1}{x+1}\right) \ .\end{aligned} \tag{113}$$

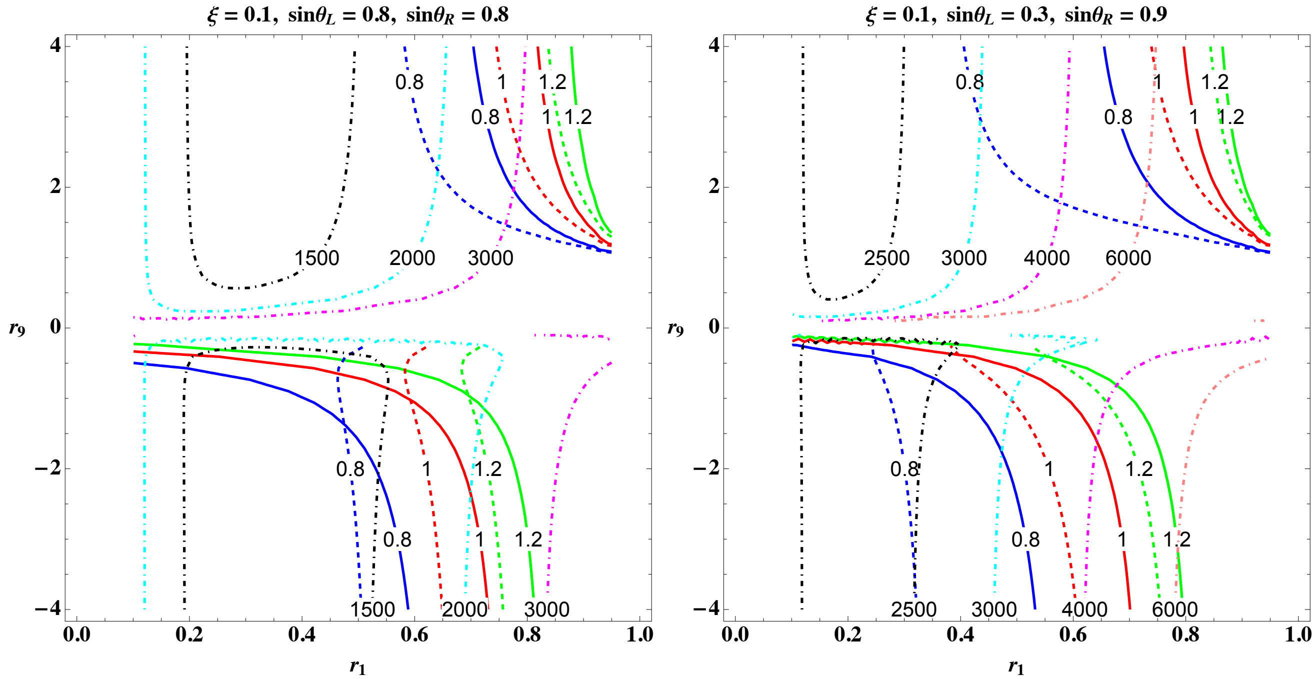

FIG. 5: The contour plots for c_g (in solid lines) , c_t (in dashed lines) and $|M_4|[\,\mathrm{GeV}]$ (in dotted dashed lines). All plots use the full formulas in Eq. (8), Eq. (15) and Eq. (16) in the case of **14** and M_4 is determined by the top mass $m_t = 150$ GeV.

Again $\mathcal{F}(x) > 0$ through out the integration region, $0 < x < x_\Lambda$, is a sufficient condition to trigger EWSB. Notice that the second contribution to $\mathcal{F}_1(x)$ in Eq. (113) is identical to $\mathcal{F}_1(x)$ in the case of **5** in Eq. (57)[5], apart from the numerical coefficient of 5/2. It was shown there that this contribution is quite insignificant when it is positive in the region of $1/2 < r_1^2 < 1$; see Eq. (59). The first term in $\mathcal{F}_1(x)$ is positive in the following region:

$$r_9^2 < 1, \qquad r_1^2 < r_9^2 \cos^2\theta_R, \qquad \text{or} \qquad r_9^2 > 1, \qquad r_1^2 > r_9^2 \cos^2\theta_R \tag{114}$$

and can become sizeable if $|\cos\theta_R/r_1|$ is either much smaller than 1 or much larger than 1. Actually, it is possible to prove:

$$\mathcal{F}_1(x) \leq \frac{9}{4}\sin^2\theta_L \left(1 - \left|\frac{\cos\theta_R}{r_1}\right|\right)^2 + \frac{5}{2}\left(\frac{3}{2} - \sqrt{2}\right)\sin^2\theta_L \sin^2\theta_R \ . \tag{115}$$

In Fig. 6, we perform numerical scans over $(r_1, r_9, \theta_L, \theta_R)$, with M_4 determined by the mass of m_t for $\xi = 0.1, 0.2$. In the upper plots of γ_f versus $c_t - c_g$, we see that there is a strong preference for $c_t < c_g$ to have a positive γ_f to trigger the EWSB. Although there are regions where a significant positive γ_f can be obtained for $c_t > c_g$, we show in the lower plot that, once we require that both the value of ξ and the Higgs mass $m_h = 125\,\mathrm{GeV}$ are reproduced by the Higgs potential, c_t is always less than c_g in the case of $\xi = 0.1$. Although, we find some points with $c_t > c_g$ in the case of $\xi = 0.2$, both c_t and c_g are very small < 0.5 and are not very phenomenologically interesting. Our results in Fig. 6 not only confirm the findings in Ref. [21], but also provide an analytic understanding of the strong correlation.

B. The Bottom Sector

For the bottom sector, as similar to the case of **5** and **10**, we introduce composite fermions that mix with b_R but not t_R. The form factors are almost identical to the top except that the mass scales and the mixing parameters are

---

[5] Recall that this is the singlet fermion contribution to the γ_f in the Higgs potential.

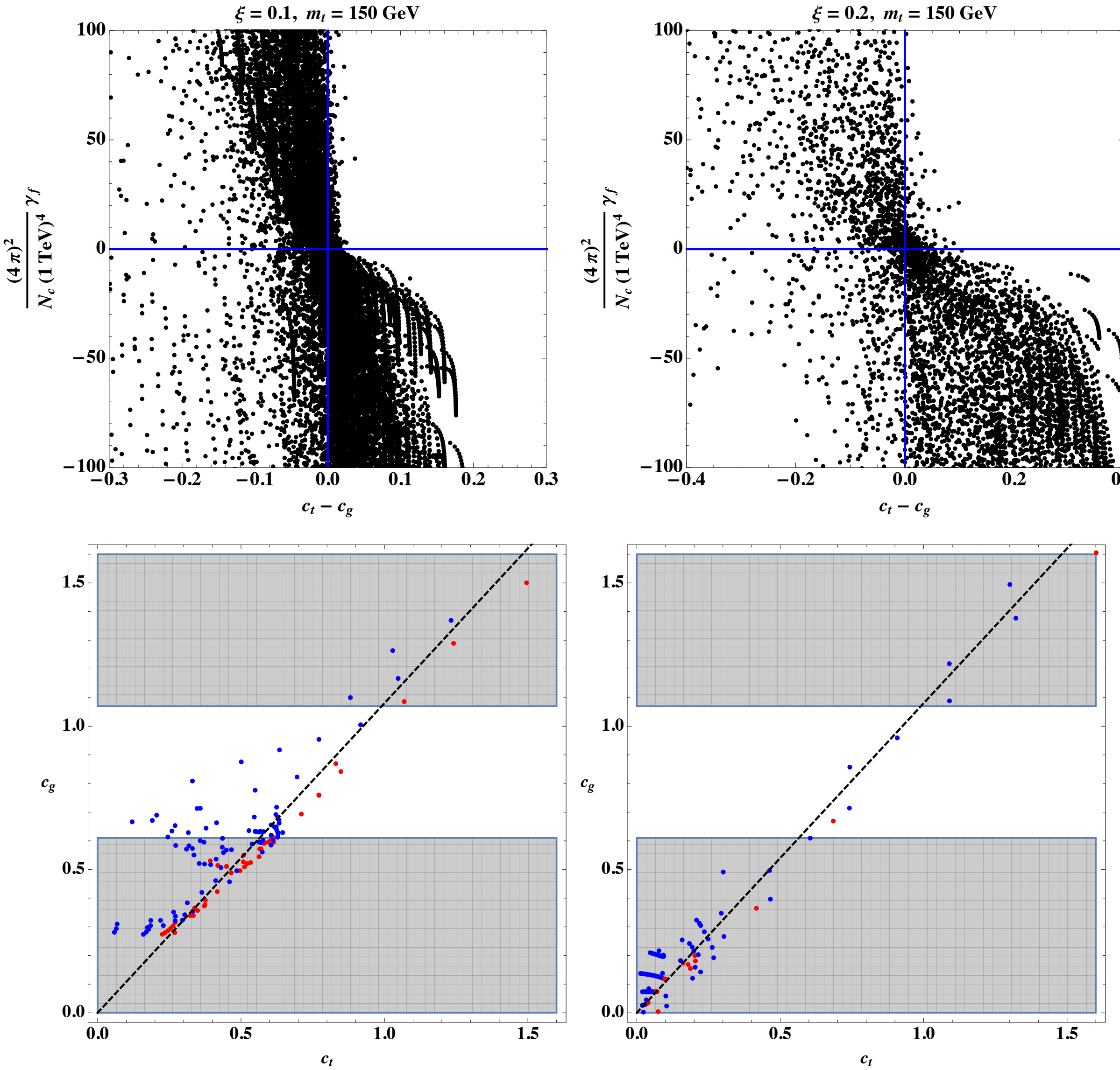

FIG. 6: Scattering plots in the case of **14** for γ_f versus $c_t - c_g$ (upper panels) without requiring the Higgs potential to reproduce the value of ξ and m_h and c_t versus c_g (lower panels) with ξ and $m_h = 125\,\text{GeV}$ correctly reproduced for $\xi = 0.1$ (left panels) and $\xi = 0.2$ (right panels). In our plots, we have required that all the mass scales including the mixing parameters $(c_4 y_L f, a_1 y_R f)$ are smaller than the cutoff $\Lambda = 4\pi f$ and the lightest top partner is heavier than 1 TeV for the upper panels. For the lower panels, the blue points are indicating that the lightest top partner mass is in the region of [500 GeV, 1TeV] and the red points are for > 1 TeV. We can see clearly that as the bounds on the top partner mass goes up, the deviation between c_t and c_g becomes smaller. The grey regions are excluded at 95% for the ggh coupling measurement at the LHC: $c_g = 0.81^{+0.13}_{-0.10}$ (see Table 17 of Ref. [3]).

now in the bottom sector. The elementary doublet q_L are "uplifted" to the $SO(5)$ space via

$$q_L^{14} = t_L P_{t_L} + b_L P_{b_L}, \qquad b_R^{14} = b_R P_{b_R} \,, \tag{116}$$

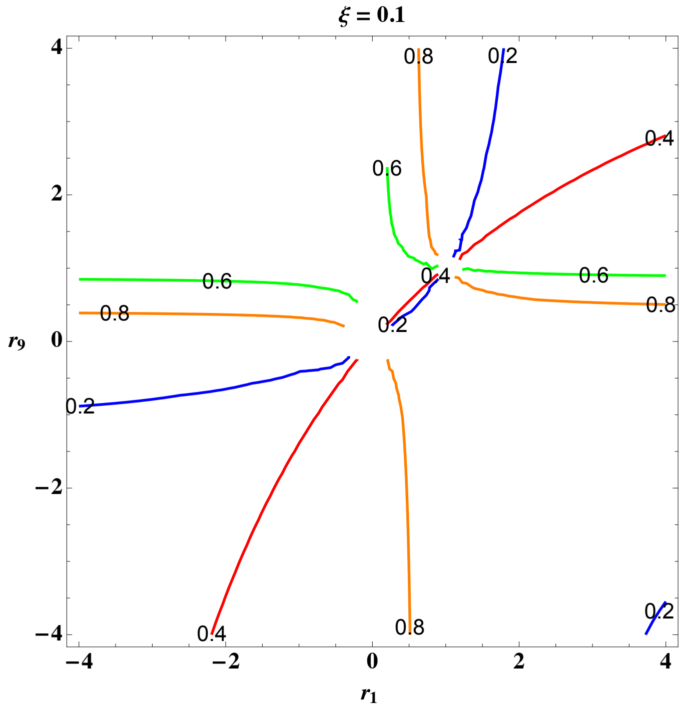

FIG. 7: Contour plots for the c_b with $\xi = 0.1$, where we have neglected all the mixing parameters in the bottom sector.

$$
\begin{aligned}
(P_{t_L})^{IJ} &= \frac{1}{2}\begin{pmatrix} & & & & -i \\ & & & & 1 \\ & & & & 0 \\ & & & & 0 \\ -i & 1 & 0 & 0 & \end{pmatrix}, \qquad (P_{b_L})^{IJ} = \frac{1}{2}\begin{pmatrix} & & & & 0 \\ & & & & 0 \\ & & & & i \\ & & & & 1 \\ 0 & 0 & i & 1 & \end{pmatrix}, \\
(P_{b_R})^{IJ} &= \frac{1}{2\sqrt{5}}\begin{pmatrix} -1 & & & & \\ & -1 & & & \\ & & -1 & & \\ & & & -1 & \\ & & & & 4 \end{pmatrix}.
\end{aligned} \tag{117}
$$

The $SO(5)$ invariants in this case are quite similar to those in the top sector,

$$
\begin{aligned}
\Sigma^T P_{b_L}^\dagger P_{b_R} \Sigma^* &= \frac{3}{4\sqrt{5}} s_h c_h \ , \qquad \Sigma^T P_{b_L}^\dagger \Sigma\ \Sigma^\dagger P_{b_R} \Sigma^* = \left(\frac{2\sqrt{5}}{5} - \frac{\sqrt{5}}{2} s_h^2\right) s_h c_h \ , \\
\Sigma^T P_{b_L}^\dagger P_{b_L} \Sigma^* &= \frac{1}{2} - \frac{1}{4} s_h^2 \ , \qquad \Sigma^T P_{b_L}^\dagger \Sigma\ \Sigma^\dagger P_{b_L} \Sigma^* = s_h^2 - s_h^4 \ , \\
\Sigma^T P_{b_R}^\dagger P_{b_R} \Sigma^* &= \frac{4}{5} - \frac{3}{4} s_h^2 \ , \qquad \Sigma^T P_{b_R}^\dagger \Sigma\ \Sigma^\dagger P_{b_R} \Sigma^* = \frac{4}{5} - 2 s_h^2 + \frac{5}{4} s_h^4 \ ,
\end{aligned} \tag{118}
$$

where the expansions in s_h^2 are evident and terminate at the s_h^4 order. The effective Lagrangian is similar to Eqs. (93) to (95), with t_R^{14} replaced by b_R^{14}.

Mixing parameters are defined similar to Eqs. (97) and (104), with all the parameters now referring to the bottom partners now. As such we still need $\sin\theta_L^{(b)}\ \sin\theta_R^{(b)} \sim 0.02$ in order to reproduce the small bottom quark mass for $\xi = 0.1$ and $M_4^{(b)} = 1$ TeV. Therefore their contribution to the Higgs potential can be ignored.

The modification to the bottom Yukawa coupling is identical to Δ_t in Eq. (107), with all the parameters referring to their counterpart in the bottom sector. On the other hand, the ggh coupling from the bottom sector is given by

$$
\Delta_g^{(b)} = -\frac{5}{2}\sin^2\theta_L^{(b)}\left(1 - \frac{1}{2}\frac{1}{(r_9^{(b)})^2} - \frac{1}{2}\frac{1}{(r_1^{(b)})^2}\right) - \frac{5}{2}\sin^2\theta_R^{(b)}\left(1 - (r_1^{(b)})^2\right) \ , \tag{119}
$$

$\xi=\frac{v^2}{f^2}$	**5**	**10**	**14**	**5 + 10**
c_g	$1-\frac{3}{2}\xi$	$1+\xi\left[-\frac{3}{2}+\left(\frac{1}{r_6^2}-1\right)\sin^2\theta_L\right]$	$1+\xi\left[-4-\frac{3}{2}\frac{1-1/r_9}{1-1/r_1}+\left(\frac{1}{r_9^2}-1\right)\sin^2\theta_L\right]$	Eq. (D4)
c_t	$<1-\frac{1}{2}\xi$	$<1-\xi$	no bound	no bound
c_b	$<1-\frac{1}{2}\xi$	$<1-\xi$	no bound	no bound
c_t-c_g	$<\xi$	$<\frac{3}{2}\xi$	$<\frac{7}{2}\xi$	$<\xi$

TABLE I: Summary for the leading contribution to c_g, c_t, c_b and c_t-c_g for the case of $\mathbf{5},\mathbf{10},\mathbf{14},\mathbf{5}+\mathbf{10}$, where in c_g we only include the top sector contribution. For the case of $\mathbf{5}+\mathbf{10}$, we only consider the case that only t_R is mixing with both **5** and **10** and q_L is only mixing with **5**.

which is quite different from Eq. (106) because we have to subtract the SM bottom contribution. In Fig. 7, we plot the contours of c_b with $\xi=0.1$ neglecting all the mixing parameters in the bottom sector. Due to the dependence on ratios of the mass scales, c_b can be suppressed significantly. A phenomenological fit to current Higgs data at the LHC is left for future work.

V. CONCLUSIONS

In this work we studied patterns of modifications in the Higgs couplings to third generation quarks and to two gluons in the $SO(5)/SO(4)$ minimal composite Higgs model. These three couplings play crucial roles in determining phenomenology of the Higgs boson at the LHC. We first presented a general framework for computing the aforementioned couplings by integrating out, at the leading order, partners of the third generation quarks, which is justified as the present searches for the vector-like quark will roughly push the mass scale to 1 TeV. Then we applied the computation to three scenarios where the composite fermions are embedded in **5**, **10** and **14** of $SO(5)$. We also computed the contribution to the Coleman-Weinberg potential of the Higgs boson from the top sector and demonstrated a strong correlation between the $t\bar{t}h$ and the ggh couplings regions of parameter space where the electroweak symmetry breaking is triggered radiatively by the top sector.

Our findings are summarized in Table I. The interesting patterns are

- the $t\bar{t}h$ and $b\bar{b}h$ couplings are always reduced relative to their SM expectations if the composite fermions are embedded in **5** or **10**, while these couplings can be either enhanced or suppressed in **14** or **5 + 10**.
- the ggh coupling is always suppressed and independent of the mass scale of the top partner in **5**. Such a pattern does not hold for embeddings in other representations.
- There exists strong correlations between c_t and c_g, assuming the top sector gives the dominant contribution to the Coleman-Weinberg potential of the Higgs boson. In regions of parameter space where the electroweak symmetry is triggered, $c_t<c_g$ is strongly preferred. Since the SM gauge boson contributions to the Higgs potential will always tend to preserve the electroweak symmetry, including them will make the preference even stronger.

These patterns could serve as diagnostic tools should a significant deviation appear in future Higgs measurements. In the absence of deviations, they can be used to potentially constrain the size of $\xi=v^2/f^2$ in the $SO(5)/SO(4)$ composite Higgs models. The Higgs coupling measurements at the LHC Run-I roughly put bound of $\xi\lesssim 0.2$ and the HL-LHC (3 ab^{-1}) is sensitive to the value of ξ as small as 0.05. The precision measurement on $c_g(c_t)$ at the HL-LHC will be roughly 3%(7%) (see Ref. [34]) and if a significant deviation between c_t and c_g were observed, with the pattern $c_t>c_g$, an additional source of EWSB, besides the one associated with the top quark, would be necessary in the minimal composite models considered in this article.

It should be emphasized that we have only considered the minimal coset structure of $SO(5)/SO(4)$. Obviously minimality is not always the best guideline when it comes to Nature. In particular, we have assumed through out this work that the dominant contribution to the Coleman-Weinberg potential arises from the top sector. It is conceivable that, if one introduces an additional contribution to the Higgs potential to trigger the EWSB, one could then weakened the strong correlation between c_t and c_g. One such possibility is to enlarge the coset structure to include an $U(1)_A$ gauge boson, like in the original Georgi-Kaplan model in Refs. [10, 11]. We hope to return to such a scenario in the future.

Acknowledgments

Work at University of Chicago is supported in part by U.S. Department of Energy grant number DE-FG02-13ER41958. Work at ANL is sup- ported in part by the U.S. Department of Energy under Contract No. DE-AC02-06CH11357. I.L. is supported in part by the U.S. Department of Energy under Contract No. DE-SC0010143.

Appendix A: CCWZ for SO(5)/SO(4)

We present here our basis for the generators of the $SO(5)$ and $SO(4)$ generators, and review the CCWZ formalism for the $SO(5)/SO(4)$ coset. The $SO(5)$ generators are defined as:

$$T^{\hat{a}}_{IJ} = -\frac{i}{\sqrt{2}}(\delta^{\hat{a}I}\delta^{5J} - \delta^{\hat{a}J}\delta^{5I}), \tag{A1}$$

$$\begin{aligned} T^{aL/R}_{IJ} &= -\frac{i}{2}\left(\frac{1}{2}\epsilon^{abc}(\delta^{bI}\delta^{cJ} - \delta^{bJ}\delta^{cI}) \pm (\delta^{aI}\delta^{4J} - \delta^{aJ}\delta^{4I})\right) \\ &= -\frac{i}{2}\left(\epsilon^{abc}\delta^{bI}\delta^{cJ} \pm (\delta^{aI}\delta^{4J} - \delta^{aJ}\delta^{4I})\right) . \end{aligned} \tag{A2}$$

where $\hat{a} = 1, \cdots, 4$, $a, b, c = 1, 2, 3$ and $I, J = 1, \cdots, 5$. In Eq. (A2) the T^L (T^R) generators take the plus (minus) sign. The generators satisfy Tr $T^A T^B = \delta^{AB}$ as well as the following commutation relations:

$$[T^{aL}, T^{bL}] = i\epsilon^{abc}T^{cL}, \quad [T^{aR}, T^{bR}] = i\epsilon^{abc}T^{cR}, \quad [T^{aL}, T^{bR}] = 0, \quad [T^a, T^{\hat{a}}] = t^a_{\hat{b}\hat{a}}T^{\hat{b}} . \tag{A3}$$

The generators $T^{a\,L}$ and $T^{a\,R}$ correspond to the unbroken $SO(4) \simeq SU(2)_L \times SU(2)_R$ generators.

The Goldstone matrix is defined as $U = e^{i\Pi}$, where the Goldstone fields Π are given by:

$$\Pi = \frac{\sqrt{2}h^{\hat{a}}}{f}T^{\hat{a}} = \frac{-i}{f}\begin{pmatrix} 0 & \vec{h} \\ -\vec{h}^T & 0 \end{pmatrix} \tag{A4}$$

where the factor $\sqrt{2}$ is just a convention and can be absorbed by the redefinition of decay constant f. The fourplet $\vec{h}$ can be related with the doublet notation H as follows:

$$\vec{h} = \frac{1}{\sqrt{2}}\begin{pmatrix} -i(h_u - h_u^\dagger) \\ h_u + h_u^\dagger \\ i(h_d - h_d^\dagger) \\ h_d + h_d^\dagger \end{pmatrix}, \qquad H = \begin{pmatrix} h_u \\ h_d \end{pmatrix} \tag{A5}$$

from which, we can see that the fourth component of $\vec{h}$ will be our physical Higgs boson in the unitary gauge. The matrix U transforms under the non-linearly realized $SO(5)$ as follows:

$$U \to g\,U\,h^\dagger(x) \tag{A6}$$

where $g \in SO(5), h(x) \in SO(4)$. The CCWZ covariant objects d_μ, E_μ are defined as:

$$-iU^\dagger D_\mu U = -iU^\dagger\partial_\mu U + U^\dagger A_\mu U = d^{\hat{a}}_\mu T^{\hat{a}} + E^a_\mu T^a = d_\mu + E_\mu \tag{A7}$$

which transform under the non-linearly realized $SO(5)$:

$$\begin{aligned} d_\mu &\to h(x)\ d_\mu\ h(x)^\dagger \\ E_\mu &\to h(x)\ E_\mu\ h(x)^\dagger - ih(x)\partial_\mu h(x)^\dagger \end{aligned} \tag{A8}$$

Note that E_μ transforms like a gauge field under $SO(5)$. The leading two-derivative effective Lagrangian for the Goldstone bosons is

$$\frac{1}{4}f^2(d^{\hat{a}}_\mu)^2 = \frac{1}{2}(\partial_\mu h)^2 + \frac{1}{2}\frac{f^2\sin^2(\theta + h/f)}{4}(W^a_\mu - \delta^{a3}B_\mu)^2 \tag{A9}$$

where $\theta = \langle h\rangle/f$. By computing the W boson mass we see $v = f\sin\theta = 246$ GeV. In addition the hWW and hZZ couplings are given by

$$c_W = g_{hWW}/(g_{hWW})_{SM} = \sqrt{1-\xi}, \qquad c_Z = g_{hZZ}/(g_{hZZ})_{SM} = \sqrt{1-\xi}\ , \tag{A10}$$

where $\xi = v^2/f^2$. For convenience we use a non-canonical basis for the gauge bosons, which are not relevant in our analysis.

Appendix B: Partial Compositeness and The ggh coupling

In this appendix, we review the general formula for the ggh coupling induced by the composite resonances under the assumption of *partial compositeness*. We are working in the fermion mass eigenstates, whose interactions with Higgs are parametrized as (see Ref. [28, 29]):

$$-\Delta\mathcal{L} = \sum_i M_i(\langle h\rangle)\bar{\psi}_i\psi_i + \sum_{ij} Y_{ij}\bar{\psi}_i\psi_j h \tag{B1}$$

where $\langle h\rangle$ is the vacuum expectation value of the neutral Higgs boson and Y is a Hermitian matrix assumed to be real and symmetric. The partonic cross section for $gg \to h$ can be obtained by direct calculation [35]:

$$\hat{\sigma}_{gg\to h} = \frac{\alpha_s^2 m_h^2}{576\pi}\left|\sum_i \frac{Y_{ii}}{M_i}A_{1/2}(\tau_i)\right|^2 \delta(\hat{s} - m_h^2) \tag{B2}$$

where $\tau_i \equiv m_h^2/(4M_i^2)$ and fermion loop function $A_{1/2}(\tau)$ is defined as

$$A_{1/2}(\tau) \;=\; \frac{3}{2}\left[\tau + (\tau-1)f(\tau)\right]\tau^{-2} \;, \tag{B3}$$

$$f(\tau) \;=\; \begin{cases} [\arcsin\sqrt{\tau}]^2, & (\tau \leq 1), \\ -\frac{1}{4}\left[\log\frac{1+\sqrt{1-\tau^{-1}}}{1-\sqrt{1-\tau^{-1}}} - i\pi\right]^2, & (\tau > 1) \end{cases} \tag{B4}$$

and goes to 1 in the limit of $\tau \to 0$:

$$A_{1/2}(\tau \to 0) \to 1. \tag{B5}$$

We define the ggh coupling as:

$$g_{ggh} = \sum_i \frac{Y_{ii}}{M_i}A_{1/2}(\tau_i). \tag{B6}$$

It is a very good approximation to include only heavy quarks with masses heavier than the Higgs boson in the loop function. In other words, the ggh effective coupling is dominated by the sum over Y_{ii}/M_i with $M_i \gg m_h$ [18]:

$$\begin{aligned} \sum_{M_i > m_h}\frac{Y_{ii}}{M_i} &= \sum_i \frac{Y_{ii}}{M_i} - \sum_{M_i < m_h}\frac{Y_{ii}}{M_i} \\ &= \frac{1}{2}\frac{\partial}{\partial\langle h\rangle}\log\,\mathrm{Det}(M^\dagger M) - \sum_{M_i<m_h}\frac{Y_{ii}}{M_i} \;, \end{aligned} \tag{B7}$$

where we have used $Y_{ii} = \partial M_i/\partial\langle h\rangle$. Note that in our convention, the SM quark Yukawa coupling satisfies $(Y_q/M_q)_{SM} = 1/v$, where $v = 246\,\mathrm{GeV}$ is the SM Higgs VEV. Since we work in the large top mass limit and neglect all the lighter quark contributions in the SM, we have $(g_{ggh})_{\mathrm{SM}} = 1/v$. Throughout this work we define the ratio

$$c_g = \frac{g_{hgg}}{(g_{hgg})_{\mathrm{SM}}} = \frac{v}{2}\frac{\partial}{\partial\langle h\rangle}\log\,\mathrm{Det}(M^\dagger M) - v\sum_{M_i<m_h}\frac{Y_{ii}}{M_i} \;. \tag{B8}$$

For the charge 2/3 particles including the top and assuming the mass matrix is real the result simply reads

$$c_g^{(2/3)} = \sin\theta\frac{\partial}{\partial\theta}\log\,\mathrm{Det}\;M_{2/3} \;, \tag{B9}$$

where $v = f\sin\theta =$ and $\theta = \langle h\rangle/f$. For the charge -1/3 particles, we need to to extract the contribution from the SM bottom quark,

$$c_g^{(-1/3)} = \sin\theta\frac{\partial}{\partial\theta}(\log\,\mathrm{Det}\;M_{-1/3} - \log m_b) \;. \tag{B10}$$

Appendix C: Effective Lagrangian After Integrating Out The Top Partners

In this appendix we present the formula for the effective Lagrangian obtained from integrating out the composite fields, for the SM quark (q_L, t_R, b_R). The Lagrangian in the momentum space for the composite partners and the mixing terms can be generally written as:

$$\mathcal{L} = \bar{\Psi}_i(\not{p} - M_\Psi)\Psi^i + K_i^\dagger \Psi^i + \bar{\Psi}_i K^i \tag{C1}$$

where we have neglected all gauge interactions. Here i generally denotes the indices of the irreducible representations of the unbroken $SO(4)$ and K^i is constructed with the Goldstone matrix U and the elementary quark fields (q_L, t_R, b_R). The effective Lagrangian after integrating out the top partners by using the equation of motion is simply:

$$\mathcal{L}_{eff} = -\frac{K_i^\dagger(\not{p} + M_\Psi)K^i}{p^2 - M_\Psi^2} \ . \tag{C2}$$

Note that for two-indices tensor representation of $SO(4)$, the indices should be contracted as $K_{ij}^\dagger \cdots K^{ji}$, which only have effects for anti-symmetric representation.

Appendix D: $\mathbf{5} + \mathbf{10}$

In this appendix, we discuss succinctly the case where the elementary quark fields $q = (t_L, b_L, t_R, b_R)$ are mixing with both **5** and **10** at the same time. We find there is a new $SO(5)$ invariant $P_q^{5\dagger} P_q^{10} \Sigma^*$ and, as a consequence, the ggh and the quark Yukawa couplings are both dependent on the ratios of the composite scales as in the case of **14**.

In the top sector, we will consider the scenario where t_R mixes with composite resonances from both the **5** and the **10**, while $q_L = (t_L, b_L)^T$ only mixes with those in the **5**. There are other possibilities for the mixing pattern which will not be pursued here. The effective Lagrangian is:

$$\begin{aligned}
\mathcal{L}^{M1_5} &= \bar{\Psi}_{\mathbf{1}}(\not{p} - M_1)\Psi_{\mathbf{1}} + \left[c_1 y_L f(\bar{q}_L^5)_I U^I{}_5 \Psi_{\mathbf{1}R} + a_1 y_R f(\bar{t}_R^5)_I U^I{}_5 \Psi_{\mathbf{1}L} + h.c.\right] \\
\mathcal{L}^{M6_{10}} &= \bar{\Psi}_{\mathbf{6}}(\not{p} - M_6)\Psi_{\mathbf{6}} + \left[a_6 y_R f(\bar{t}_R^{10})_{IJ} U^I{}_i U^J{}_j \Psi_{\mathbf{6}L}^{ij} + h.c.\right] \\
\mathcal{L}^{M4_5} &= \bar{\Psi}_{\mathbf{4}}(\not{p} - M_4)\Psi_{\mathbf{4}} + \cos\theta_c \left[c_4 y_L f(\bar{q}_L^5)_I U^I{}_i \Psi_{\mathbf{4}R}^i + a_4 y_R f(\bar{t}_R^5)_I U^I{}_i \Psi_{\mathbf{4}L}^i + h.c.\right] \\
&\quad - \sin\theta_c \left[\sqrt{2}\tilde{a}_4 y_R f(\bar{t}_R^{10})_{IJ} U^I{}_i U^J{}_5 \Psi_{\mathbf{4}L}^i + h.c.\right] \\
\mathcal{L}^{M4_{10}} &= \bar{\tilde{\Psi}}_{\mathbf{4}}(\not{p} - \tilde{M}_4)\tilde{\Psi}_{\mathbf{4}} + \sin\theta_c \left[c_4 y_L f(\bar{q}_L^5)_I U^I{}_i \tilde{\Psi}_{\mathbf{4}R}^i + a_4 y_R f(\bar{t}_R^5)_I U^I{}_i \tilde{\Psi}_{\mathbf{4}L}^i + h.c.\right] \\
&\quad + \cos\theta_c \left[\sqrt{2}\tilde{a}_4 y_R f(\bar{t}_R^{10})_{IJ} U^I{}_i U^J{}_5 \tilde{\Psi}_{\mathbf{4}L}^i + h.c.\right]
\end{aligned} \tag{D1}$$

where the relevant projection operators are given in Eqs. (30) and (70) for **5** and **10**, respectively. Furthermore, θ_c is mixing angle between the 4-plet from the **5** and the 4-plet from the **10**. In addition to the invariants presented in Eq. (33) and Eq. (73), we have the following invariants constructed with embedding vectors $P_q^{5\dagger}, P_q^{10}$:

$$\begin{aligned}
P_{t_L}^{5\dagger} P_{t_L}^{10}\Sigma^* &= P_{b_L}^{5\dagger} P_{b_L}^{10}\Sigma^* = \frac{c_h}{\sqrt{2}}, \quad & P_{t_L}^{5\dagger} P_{t_R}^{10}\Sigma^* &= -\frac{s_h}{2\sqrt{2}}, \\
P_{t_R}^{5\dagger} P_{t_L}^{10}\Sigma^* &= \frac{s_h}{2}, & P_{t_R}^{5\dagger} P_{t_R}^{10}\Sigma^* &= 0 \ .
\end{aligned} \tag{D2}$$

Now it is straightforward to calculate the form factors as before. After imposing the following condition for the cancellation of the quadratic divergence,

$$c_4^2 = c_1^2, \qquad a_4^2 = a_1^2, \qquad \tilde{a}_4^2 = a_6^2 \ , \tag{D3}$$

the leading modifications to the ggh and $t\bar{t}h$ coupling strengths are given by:

$$\Delta_g^{(t)} = -\frac{3}{2} + \frac{\sin\theta_c\cos\theta_c\left(\frac{M_4}{\tilde{M}_4}-1\right)}{\sin\theta_c\cos\theta_c\left(\frac{M_4}{\tilde{M}_4}-1\right) \pm \sqrt{2}\frac{M_4}{M_1} \pm \sqrt{2}\left(\cos^2\theta_c + \sin^2\theta_c\frac{M_4}{\tilde{M}_4}\right)}\ , \tag{D4}$$

$$\begin{aligned}\Delta_t &= \Delta_g^{(t)} + \frac{1}{2}\sin^2\theta_L\left(1-\frac{1}{r_1^2}\right) + \frac{\tan^2\theta_R^{(1)}}{1+\tan^2\theta_R^{(1)}+\tan^2\theta_R^{(6)}}(1-r_1^2) \\ &\quad + \frac{1}{2}\frac{\tan^2\theta_R^{(6)}}{1+\tan^2\theta_R^{(1)}+\tan^2\theta_R^{(6)}}\left(1-\sin^2\theta_c\frac{M_6^2}{M_4^2}-\cos^2\theta_c\frac{M_6^2}{\tilde{M}_4^2}\right)\ ,\end{aligned} \tag{D5}$$

where the two $\pm$ sign in the $\Delta_g^{(t)}$ are not correlated and we have also defined:

$$\begin{aligned}&\tan\theta_R^{(1)} = \frac{a_1 y_R f}{M_1}, \qquad \tan\theta_R^{(6)} = \frac{a_6 y_R f}{M_6}, \qquad r_1^2 = \cos^2\theta_c\frac{M_1^2}{M_4^2} + \sin^2\theta_c\frac{M_1^2}{\tilde{M}_4^2} \\ &\tan^2\theta_L = c_4^2 y_L^2 f^2\left(\frac{\cos^2\theta_c}{M_4^2}+\frac{\sin^2\theta_c}{\tilde{M}_4^2}\right)\ .\end{aligned} \tag{D6}$$

Similar to the case of **14**, there is enough degree of freedom such that both Δ_g and Δ_t can be positive or negative. It is not difficult to see that :

$$\begin{aligned}\Delta_t - \Delta_g^{(t)} &< \frac{1}{2}\sin^2\theta_L\left(1-\frac{1}{r_1^2}\right) + \frac{\tan^2\theta_R^{(1)}}{1+\tan^2\theta_R^{(1)}+\tan^2\theta_R^{(6)}}(1-r_1^2) + \frac{1}{2}\frac{\tan^2\theta_R^{(6)}}{1+\tan^2\theta_R^{(1)}+\tan^2\theta_R^{(6)}} \\ &< \left(\frac{|\sin\theta_L|}{\sqrt{2}} - \frac{|\tan\theta_R^{(1)}|}{\sqrt{1+\tan^2\theta_R^{(1)}+\tan^2\theta_R^{(6)}}}\right)^2 + \frac{1}{2}\frac{\tan^2\theta_R^{(6)}}{1+\tan^2\theta_R^{(1)}+\tan^2\theta_R^{(6)}} \\ &< \text{Max}\left[\frac{1}{2}\sin^2\theta_L, \frac{\tan^2\theta_R^{(1)}}{1+\tan^2\theta_R^{(1)}+\tan^2\theta_R^{(6)}}\right] + \frac{1}{2}\frac{\tan^2\theta_R^{(6)}}{1+\tan^2\theta_R^{(1)}+\tan^2\theta_R^{(6)}} < 1\end{aligned} \tag{D7}$$

In the bottom sector, we consider the possibilities that all elementary fields are "uplifted" to $SO(5)$ multiplets with $X = 2/3$, which means b_R should be uplifted to an $SO(5)$ vector with $T^{3R}(b_R) = -1$:

$$(P_{b_R}^{10})^{IJ} = \frac{1}{2}\begin{pmatrix} & & -1 & -i & \\ & & i & -1 & \\ 1 & -i & & & \\ i & 1 & & & \\ & & & & 0\end{pmatrix}\ , \tag{D8}$$

and the embedding vectors for the left-handed fields are the same as the top sector. We consider the case that the left-handed quark doublet q_L is mixing with both **5** and **10**. The invariants involving the right-handed bottom quarks are listed as follows:

$$\Sigma^T P_{b_R}^{10\dagger} P_{b_R}^{10}\Sigma^* = \frac{s_h^2}{2}, \qquad \Sigma^T P_{b_L}^{10\dagger} P_{b_R}^{10}\Sigma^* = -\frac{s_h c_h}{2}, \qquad P_{b_L}^{5\dagger} P_{b_R}^{10}\Sigma^* = -\frac{s_h}{\sqrt{2}}\ . \tag{D9}$$

For simplicity we impose a similar condition to Eq. (D3) to cancel the quadratic divergence in the bottom sector. The modification to the bottom Yukawa coupling is given by

$$\Delta_b \sim -\frac{3}{2} + \frac{\sin\theta_c^{(b)}\cos\theta_c^{(b)}\left(\frac{M_4^{(b)}}{\tilde{M}_4^{(b)}}-1\right)}{\sin\theta_c^{(b)}\cos\theta_c^{(b)}\left(\frac{M_4^{(b)}}{\tilde{M}_4^{(b)}}-1\right) \pm \left(\sin^2\theta_c^{(b)} + \cos^2\theta_c^{(b)}\frac{M_4^{(b)}}{\tilde{M}_4^{(b)}}\right) \pm \frac{M_4^{(b)}}{M_6^{(b)}}} \tag{D10}$$

where the two $\pm$ signs are not correlated with each other and we have neglected the mixing angles in the bottom sector. Similar to the case of **14**, there is enough degree of freedom to suppress bottom Yukawa coupling as needed.

---

[1] **ATLAS** Collaboration, G. Aad *et al.*, "Observation of a new particle in the search for the Standard Model Higgs boson with the ATLAS detector at the LHC," *Phys. Lett.* **B716** (2012) 1–29, `arXiv:1207.7214 [hep-ex]`.

[2] **CMS** Collaboration, S. Chatrchyan *et al.*, "Observation of a new boson at a mass of 125 GeV with the CMS experiment at the LHC," *Phys. Lett.* **B716** (2012) 30–61, `arXiv:1207.7235 [hep-ex]`.

[3] **ATLAS, CMS** Collaboration, G. Aad *et al.*, "Measurements of the Higgs boson production and decay rates and constraints on its couplings from a combined ATLAS and CMS analysis of the LHC pp collision data at $\sqrt{s} = 7$ and 8 TeV," *JHEP* **08** (2016) 045, `arXiv:1606.02266 [hep-ex]`.

[4] S. P. Martin, "A Supersymmetry primer," `arXiv:hep-ph/9709356 [hep-ph]`. [Adv. Ser. Direct. High Energy Phys.18,1(1998)].

[5] J. F. Gunion and H. E. Haber, "Higgs Bosons in Supersymmetric Models. 1.," *Nucl. Phys.* **B272** (1986) 1. [Erratum: Nucl. Phys.B402,567(1993)].

[6] M. Badziak and C. E. M. Wagner, "Enhancing the Higgs associated production with a top quark pair," *JHEP* **05** (2016) 123, `arXiv:1602.06198 [hep-ph]`.

[7] M. Badziak and C. E. M. Wagner, "Enhanced Higgs associated production with a top quark pair in the NMSSM with light singlets," `arXiv:1611.02353 [hep-ph]`.

[8] H. Terazawa, K. Akama, and Y. Chikashige, "Unified Model of the Nambu-Jona-Lasinio Type for All Elementary Particle Forces," *Phys. Rev.* **D15** (1977) 480.

[9] H. Terazawa, "Subquark Model of Leptons and Quarks," *Phys. Rev.* **D22** (1980) 184.

[10] D. B. Kaplan and H. Georgi, "SU(2) x U(1) Breaking by Vacuum Misalignment," *Phys. Lett.* **B136** (1984) 183–186.

[11] D. B. Kaplan, H. Georgi, and S. Dimopoulos, "Composite Higgs Scalars," *Phys. Lett.* **B136** (1984) 187–190.

[12] N. Arkani-Hamed, A. G. Cohen, and H. Georgi, "Electroweak symmetry breaking from dimensional deconstruction," *Phys. Lett.* **B513** (2001) 232–240, `arXiv:hep-ph/0105239 [hep-ph]`.

[13] N. Arkani-Hamed, A. G. Cohen, E. Katz, A. E. Nelson, T. Gregoire, and J. G. Wacker, "The Minimal moose for a little Higgs," *JHEP* **08** (2002) 021, `arXiv:hep-ph/0206020 [hep-ph]`.

[14] N. Arkani-Hamed, A. G. Cohen, E. Katz, and A. E. Nelson, "The Littlest Higgs," *JHEP* **07** (2002) 034, `arXiv:hep-ph/0206021 [hep-ph]`.

[15] R. Contino, Y. Nomura, and A. Pomarol, "Higgs as a holographic pseudoGoldstone boson," *Nucl. Phys.* **B671** (2003) 148–174, `arXiv:hep-ph/0306259 [hep-ph]`.

[16] K. Agashe, R. Contino, and A. Pomarol, "The Minimal composite Higgs model," *Nucl. Phys.* **B719** (2005) 165–187, `arXiv:hep-ph/0412089 [hep-ph]`.

[17] Y. Hosotani, "Dynamics of Nonintegrable Phases and Gauge Symmetry Breaking," *Annals Phys.* **190** (1989) 233.

[18] A. Falkowski, "Pseudo-goldstone Higgs production via gluon fusion," *Phys. Rev.* **D77** (2008) 055018, `arXiv:0711.0828 [hep-ph]`.

[19] I. Low, R. Rattazzi, and A. Vichi, "Theoretical Constraints on the Higgs Effective Couplings," *JHEP* **04** (2010) 126, `arXiv:0907.5413 [hep-ph]`.

[20] I. Low and A. Vichi, "On the production of a composite Higgs boson," *Phys. Rev.* **D84** (2011) 045019, `arXiv:1010.2753 [hep-ph]`.

[21] M. Montull, F. Riva, E. Salvioni, and R. Torre, "Higgs Couplings in Composite Models," *Phys. Rev.* **D88** (2013) 095006, `arXiv:1308.0559 [hep-ph]`.

[22] M. Carena, L. Da Rold, and E. Ponton, "Minimal Composite Higgs Models at the LHC," *JHEP* **06** (2014) 159, `arXiv:1402.2987 [hep-ph]`.

[23] A. Falkowski, "About the holographic pseudo-Goldstone boson," *Phys. Rev.* **D75** (2007) 025017, `arXiv:hep-ph/0610336 [hep-ph]`.

[24] A. D. Medina, N. R. Shah, and C. E. M. Wagner, "Gauge-Higgs Unification and Radiative Electroweak Symmetry Breaking in Warped Extra Dimensions," *Phys. Rev.* **D76** (2007) 095010, `arXiv:0706.1281 [hep-ph]`.

[25] D. B. Kaplan, "Flavor at SSC energies: A New mechanism for dynamically generated fermion masses," *Nucl. Phys.* **B365** (1991) 259–278.

[26] I. Low, "Minimally symmetric Higgs boson," *Phys. Rev.* **D91** no. 11, (2015) 116005, `arXiv:1412.2146 [hep-ph]`.

[27] K. Agashe, R. Contino, L. Da Rold, and A. Pomarol, "A Custodial symmetry for $Zb\bar{b}$," *Phys. Lett.* **B641** (2006) 62–66, `arXiv:hep-ph/0605341 [hep-ph]`.

[28] A. Azatov and J. Galloway, "Light Custodians and Higgs Physics in Composite Models," *Phys. Rev.* **D85** (2012) 055013, `arXiv:1110.5646 [hep-ph]`.

[29] E. Furlan, "Gluon-fusion Higgs production at NNLO for a non-standard Higgs sector," *JHEP* **10** (2011) 115, `arXiv:1106.4024 [hep-ph]`.

[30] R. Contino, "The Higgs as a Composite Nambu-Goldstone Boson," in *Physics of the large and the small, TASI 09, proceedings of the Theoretical Advanced Study Institute in Elementary Particle Physics, Boulder, Colorado, USA, 1-26 June 2009*, pp. 235–306. 2011. `arXiv:1005.4269 [hep-ph]`.

http://inspirehep.net/record/856065/files/arXiv:1005.4269.pdf.
[31] S. R. Coleman, J. Wess, and B. Zumino, "Structure of phenomenological Lagrangians. 1.," *Phys. Rev.* **177** (1969) 2239–2247.
[32] C. G. Callan, Jr., S. R. Coleman, J. Wess, and B. Zumino, "Structure of phenomenological Lagrangians. 2.," *Phys. Rev.* **177** (1969) 2247–2250.
[33] C. Csaki, T. Ma, and J. Shu, "The Maximally Symmetric Composite Higgs," arXiv:1702.00405 [hep-ph].
[34] S. Dawson *et al.*, "Working Group Report: Higgs Boson," in *Proceedings, 2013 Community Summer Study on the Future of U.S. Particle Physics: Snowmass on the Mississippi (CSS2013): Minneapolis, MN, USA, July 29-August 6, 2013*. 2013. arXiv:1310.8361 [hep-ex]. http://inspirehep.net/record/1262795/files/arXiv:1310.8361.pdf.
[35] J. R. Ellis, M. K. Gaillard, and D. V. Nanopoulos, "A Phenomenological Profile of the Higgs Boson," *Nucl. Phys.* **B106** (1976) 292.